Ore Geology Reviews 113 (2019) 103073

Contents lists available at ScienceDirect

Ore Geology Reviews

journal homepage: www.elsevier.com/locate/oregeorev

Geochemistry, mineralogy and genesis of rare metal (Nb-Ta-Zr-Hf-Y-REE-Ga) coals of the seam XI in the south of Kuznetsk Basin, Russia

S.I. Arbuzov[a,*], D.A. Spears[b], A.V. Vergunov[a], S.S. Ilenok[a], A.M. Mezhibor[a], V.P. Ivanov[a], N.A. Zarubina[c]

[a] Tomsk Polytechnic University, Tomsk, Russia
[b] University of Sheffield, S10 2TN, UK
[c] Far East Geological Institute, FEB of RAS, Vladivostok, Russia

ARTICLE INFO

Keywords:
Coal basin
Nb(Ta)-Zr(Hf)-REE-Ga deposit
Pyroclastic origin
Kuzbass
Russia

ABSTRACT

The research describes the detailed mineralogical and geochemical characteristics of rare-metal Nb-Ta-Zr-Hf-Y-REE-Ga ores found in Permian coals in the layer XI in the south of the Kuznetsk Basin. The concentrations and distribution of ore, and related elements, were studied in the coal seam section and along the seam strike. Spatial and genetic relationships of the mineralization in the coal were found to be related to the presence of an altered volcanogenic pyroclastic horizon of REE-enriched pantellerite composition. The highest concentrations of basic ore elements in the coal are associated with the contact zones above and below the volcanogenic horizon. The ore matter is mainly concentrated in the fine mineral phases, composed mainly of Zr-Nb-Ti-Fe oxides, fine zircons, rare-earth carbonates (bastnesite) and phosphates (monazite, xenotime, goyacite). Resource estimates are made of the rare metals. Confirmation of the connection between the complex rare-metal mineralization and the alkaline volcanogenic pyroclastics significantly expands the prospects of revealing further such mineralization in the coals of East and Central Asia.

1. Introduction

Like its precursor peat, coal is a contrasting geochemical barrier to the accumulation of various chemical elements. Consequently coal is favourable for the formation of geochemical anomalies with the precipitation of many metals in coal seams. For more than 100 years the issue of extracting by-product impurities from coal and its utilization wastes has been attempted with varying degrees of success. Nowadays, a large group of diverse deposits of rare, noble, and nonferrous metals in coals and carbonaceous rocks is known (Seredin, 2004; Seredin and Finkelman, 2008; Seredin and Dai, 2012; Seredin et al., 2013; Arbuzov et al., 2014; Dai et al., 2018a, 2018b; Dai and Finkelman, 2018). Only germanium has been commercially extracted from coal, but more recently, lithium and gallium have been mined (Seredin, 2012; Lin et al., 2013; Qin et al., 2015).

General trends of increasing demand for rare metals and developing new processing technologies allow us to be optimistic about the prospects for the development of traditional and new types of rare-metal coal deposits. Attempts to explore new deposits are continuing. In addition to the group of germanium-coal deposits in China, such as the Lincang and Wulantuga deposits (Zhuang et al., 2006; Hu et al., 2009; Dai et al., 2012a, 2015;), several deposits of complex REY-Zr(Hf)-Nb(Ta)-Ga ores have been identified in recent years (Dai et al., 2010, 2012b). Similar rare-metal-coal deposits have been known in Kuznetsk Basin (Kuzbass) and Minusinsky Basin (Seredin, 1994; Arbuzov et al., 2000, 2003; Arbuzov and Ershov, 2007). The mineralization in the seam XI in the Kuznetsk Basin is of particular interest because of the element concentrations and the scale of the enrichment. The nature of this type of complex mineralization is interpreted in different ways: from syngenetic hydrogenic mineralization (Seredin, 1994) to volcanogenic (Arbuzov et al., 2003; Arbuzov and Ershov, 2007; Seredin and Finkelman, 2008; Dai et al., 2010, 2012b) and volcanogenic-hydrothermal ones (Dai et al., 2016; Seredin, 1994; C. Zhao et al., 2017; L. Zhao et al., 2017a, 2017b). Understanding the mechanisms of the formation of such ores and modeling their formation will aid effective prediction and reveal similar mineralization in previously unexploited areas.

In this research, the authors studied the main mineralogical and geochemical features of the complex Nb-Ta-Zr-Hf-Y-REE-Ga element association in the coal seam XI in the south of Kuzbass to establish both the nature of its formation and create a potential reference section. The element association was revealed in 1989 by V.V. Ershov (Rikhvanov

* Corresponding author.
E-mail address: siarbuzov@mail.ru (S.I. Arbuzov).

https://doi.org/10.1016/j.oregeorev.2019.103073
Received 11 June 2019; Received in revised form 12 August 2019; Accepted 15 August 2019
Available online 17 August 2019

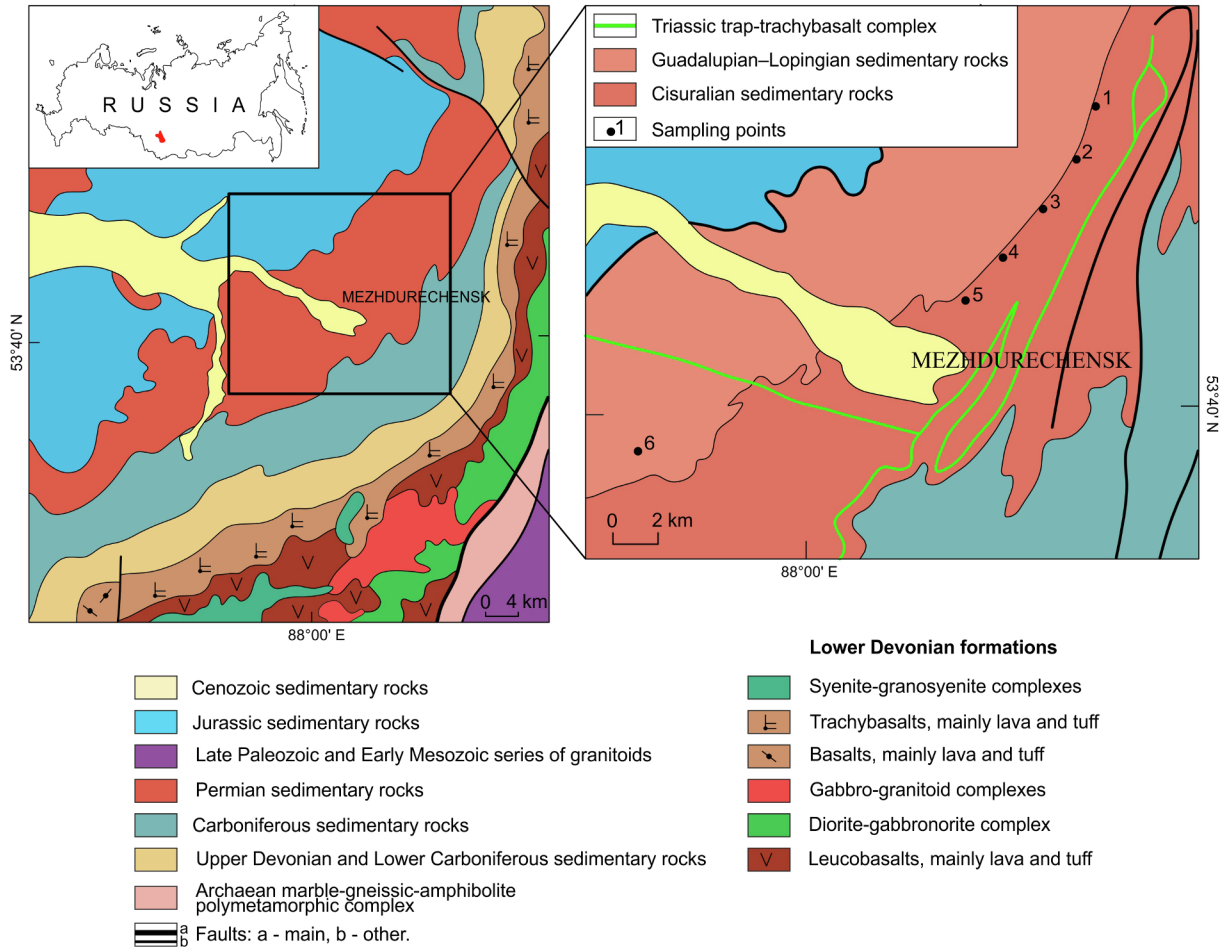

Fig. 1. A fragment of the geological map of the south of Kuzbass (Babin et al., 2007) and the position of the sampling sites of the seam XI.

et al. (1992, 1994)) and briefly described by Seredin (1994, 2004). Preliminary resource estimates were made (Arbuzov et al., 2000; Arbuzov and Ershov, 2007), and in the Sheviakov mine the estimated tantalum resources exceeded 100 tonnes. However, the complex Nb-Ta-Zr-Hf-Y-REE-Ga association in the coal seam XI was not studied in detail due to the limited technical capacity at that time.

1.1. Distribution of seam XI in the Kuznetsk Basin

The studied seam is located in the southern part of the Kuznetsk Basin close to the sediments' source area. The Kuznetsk Basin is an intermountain depression formed in Carboniferous-Permian time over the Paleozoic basement. In addition to terrigenous-carbonate sediments, there occur volcanogenic strata of predominantly basaltic and alkaline-basite composition, and diverse intrusive complexes of felsic, alkaline and mafic composition. Endogenous deposits and occurrences of non-ferrous and rare metals are widespread in the source area at the southern and southeastern margins of the coal-accumulation basin (Fig. 1).

The coal-bearing stratum in the south of Kuzbass, within which the seam XI has been identified, represents a large monocline with layers dipping to the west, while the monocline itself dips to the south-west (Yuzvitsky, 2003). In the northeastern part of the monocline, the dip of the beds is less and the thickness of the Cisuralian sediments is greater than in the southwestern part. In the northwest direction they are covered by Upper Permian coal-bearing sediments of the Guadalupian and Lopingian Series (Fig. 2).

The seam XI mainly outcrops in the south of the Kuznetsk Basin and can be traced over 50 km from east to west (Fig. 1). The seam can also be traced more than 5800-m down dip. The seam was studied in this work from the eastern part of the basin. In the west it also outcrops in the Abashevskaya mine. In the central and northern parts of the basin seam XI has not been unambiguously identified due the current lack of suitable correlations. According to preliminary data, analogues of the seam XI can be found in different coal-bearing regions of the central and northern Kuzbass, for example, the Gorely, Volkovsky, and Podvolkovsky seams. The seam XI is stratigraphically part of the Kemerovo suite deposits of the Cisuralian series of early Permian age (Fig. 2) (Yuzvitsky, 2003).

2. Research methods

2.1. Sampling

The sampling was carried out in mines (in open cuts and underground workings) over the period from 1989 to 2018. Twelve sections have been sampled in total. Two sections were sampled in the Shevyakov mine, seven sections in the Lenin mine and single sections in other mines. The most detailed section was made in 2018 in the Raspadsky open cut (Fig. 3).

The sampling was carried out by furrow method with a furrow cross-section of 15 × 5 cm. The length of the sampling sections depended on the vertical seam homogeneity and ranged from 1.5 to 10 cm in the detailed study and from 5 to 70 cm in other sections. Thirty-four samples were taken in the detailed section with the total thickness of 1.5 m. In addition to the coal, the roof and the bottom of the seam were sampled, as well as the intrastratal rock interlayers.

In the previous sampling (1989–2002), from eight to fifteen samples

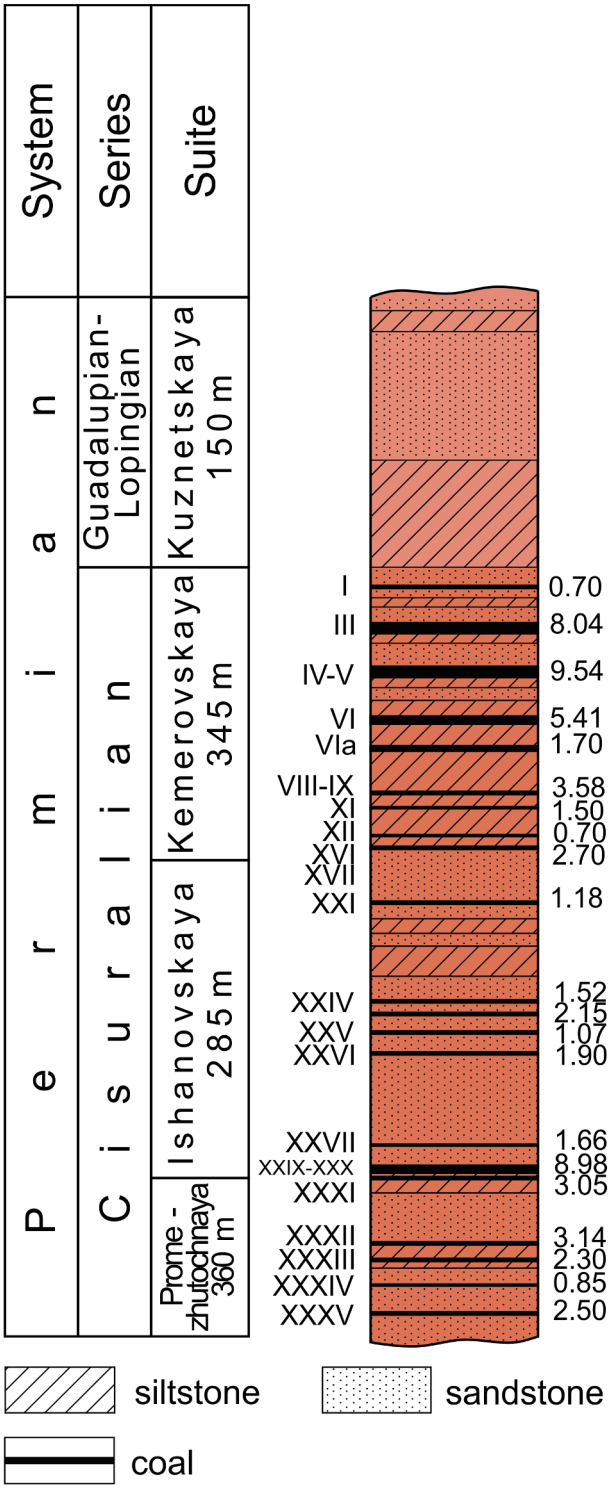

Fig. 2. Stratigraphic scheme of the coal-bearing sediment separation in the south of the Kuznetsk Basin and the position of the seam XI.

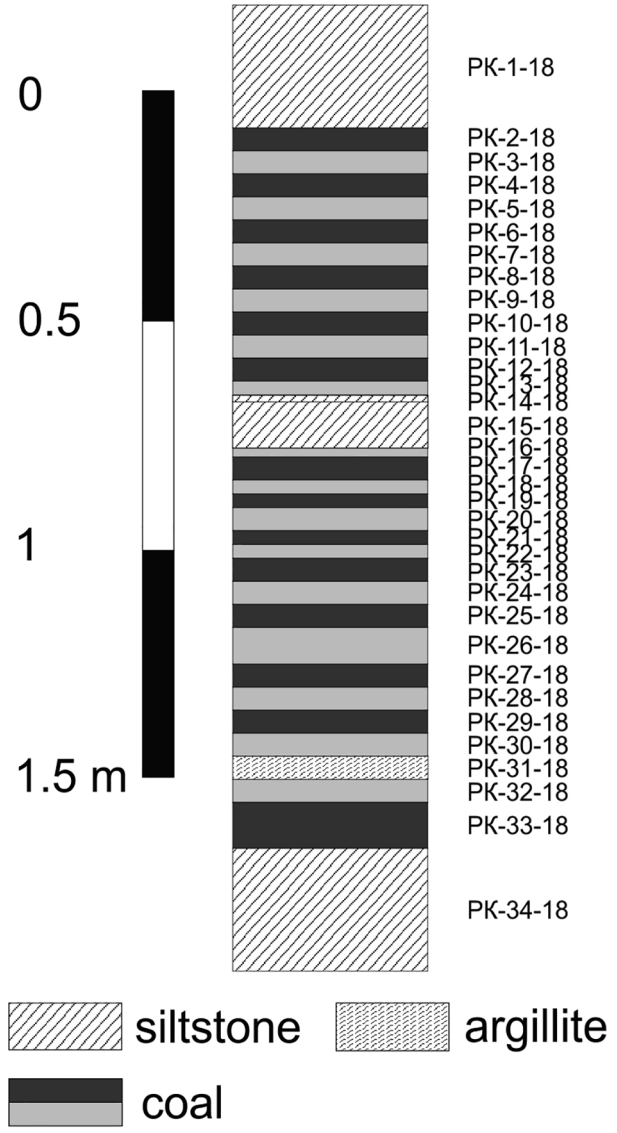

Fig.3. Scheme of the coal sampling in the seam XI in the Raspadsky open cut.

were sampled in other sections using the same method (Arbuzov et al., 2000, Arbuzov and Ershov, 2007). In 1992, the duplicates of the samples from the Shevyakov mine were transferred by B.F. Nifantov to V.V. Seredin for research (1994, 2004).

2.2. Analytical methods

Several modern analytical methods were used in the research. These include mass spectrometry with inductively coupled plasma (ICP-MS), atomic emission spectrometry with inductively coupled plasma (ICP-AES), and instrumental neutron activation analysis (INAA).

ICP-AES and ICP-MS methods (Analytical Center of the Far East Geological Institute, Vladivostok) were used in this study to determine the elemental composition of the studied samples. The samples were ground to ≤0.076 mm (200 mesh) prior to the analysis.

The major elements (Al, Ti, Fe, Ca, Mg, K, Na, and P in terms of oxides) were determined by ICP-AES within the mode of radial plasma observation on the iCAP 7600 Duo spectrometer (Thermo Scientific, USA). The content of silica in the rocks was determined by a gravimetric method after the decomposition of the studied material by fusion with anhydrous sodium carbonate (Belopolsky et al., 1974).

Trace element analysis was performed on an Agilent 7500c quadrupole ICP-MS (Agilent Technologies, Japan) for lithium metaborate fused samples and on an Agilent 7700x quadrupole ICP-MS for open-acid-digestion technique using a mixture of HF, HNO_3, and $HClO_4$. The latter approach gave us the possibility to correctly measure Ge-, Se-, Te-, As-, Sb-, and Re-forming compounds that become volatile, and Li, which was excluded when the lithium metaborate fusion technique was used. In total, 46 elements were studied by ICP MS (Be, Sc, V, Cr, Co, Ni, Cu, Zn, Ga, Ge, As, Se, Rb, Sr, Y, Zr, Nb, Mo, Ag, Cd, Sn, Sb, Te, Cs, Ba, La, Ce, Pr, Nd, Sm, Eu, Gd, Tb, Dy, Ho, Er, Tm, Yb, Lu, Hf, Ta, W, Tl, Pb,

Th and U).

The INAA analysis was undertaken at the Nuclear Geochemical Laboratory of the Geology Department of National Research Tomsk Polytechnic University (TPU) (performed by A.F. Sudyko). Weights of 200 mg for coal and 100 mg for coal ash and coal-bearing rocks were used for the element determinations. In total, 29 chemical elements (Na, Ca, Sc, Cr, Fe, Co, Zn, As, Br, Rb, Sr, Ag, Sb, Cs, Ba, La, Ce, Nd, Sm, Eu, Gd, Tb, Yb, Lu, Hf, Ta, Au, U and Th) in the coal, coal-bearing rocks, and intracoal interlayers were measured in all samples without preliminary concentrating in order to avoid potential losses during ashing. For the control, the element concentrations were simultaneously determined in the coal ash. Neutron irradiation of the samples was performed in the research reactor IRT-T of the Research Institute of Nuclear Physics of TPU.

The quality of the neutron activation analysis was monitored using various standards of coal and rock ash, including ZUK-2 standard (Kansko-Achinsky coal ash).

The mercury concentration in the samples was determined by the RA-915 + atomic absorption spectrometer with the RA915P software package (PND F 16.1:2.23-2000). Coal and rock samples were analyzed using a pyrolytic attachment PIRO-915 (pyrolysis method). The measurement range for the mass fraction of total mercury in the samples ranged from 10^{-3} ppm to 10 ppm.

To study the features of mineral substance distribution in non-coal interlayers and analyze their texture and structural features, petrographic study of thin sections was carried out using an Axioskop-40 optical microscope.

The diagnostics of the mineral matter composition in non-coal interlayers, including clay minerals, was carried out by X-ray analysis. X-ray analysis was undertaken in the Laboratory of Lithology of the Tomsk Scientific Research and Design Institute of Oil and Gas using the RIGAKU ULTIMA IV X-ray diffractometer with the implementation of X-ray film imaging in Brega-Brentano geometry (performed by E.S. Kondrashova). The diffraction patterns were taken with the following parameters: Cu anode, X-ray tube voltage of 40 kV, current of 30 mA, power of 1.2 kW, imaging speed of 1°/min, pitch of 0.02°, and imaging angles of 2Θ from 5° to 70°. To improve the quality of X-ray analysis and identification of low-content minerals, special methods of sample processing were used (Moore and Reynolds, 1997). Quantitative mineralogical analyses of the whole rock data were performed by a Rietveld analysis (Bish and Post, 1993) using PDXL and Siroquant software (Taylor, 1991)The main mineral composition in the intra-coal interlayers and coal-bearing rocks was also determined using a diffractometer "D2 Phaser" manufactured by Bruker (performed by B.R. Soktoev).

The study of micromineral forms of elements in the coal and coal ash was carried out using the scanning electron microscope (SEM) Hitachi S-3400N at the Uranium Geology Research Center at the Geology Department of TPU. The composition of inclusions was determined on a Bruker XFlash 4010/5010 energy-dispersive spectrometer for X-ray analysis. The samples were studied in low vacuum mode with a backscattered electron detector. The sampling for the subsequent SEM research was based on the INAA and ICP MS results. The main criterion for the sampling of coal and ash was the anomalous concentrations of rare elements.

Maceral composition was determined according to ISO 7404-3:2009 on the "Palam-312" microscope with a photomultiplier "HAMATSU" and software MSF-30U using briquettes made according to ISO 7404-2:2009. Quantitative calculations were performed manually on the scanning table.

The definition of maceral composition consisted of a quantitative calculation of macerals: vitrinite (Vt), semivitrinite (Sv), inertinite (I), liptinite (L) and mineral impurities (MM) in accordance with ISO 7404-3: 2009. Transitional petrographic variation between the vitrinite (Vt) and fusenite (F) in the form of the maceral semivitrinite is also designated in other countries as semifuzinite (Sf), which is permissible in the practice of coal petrography analysis.

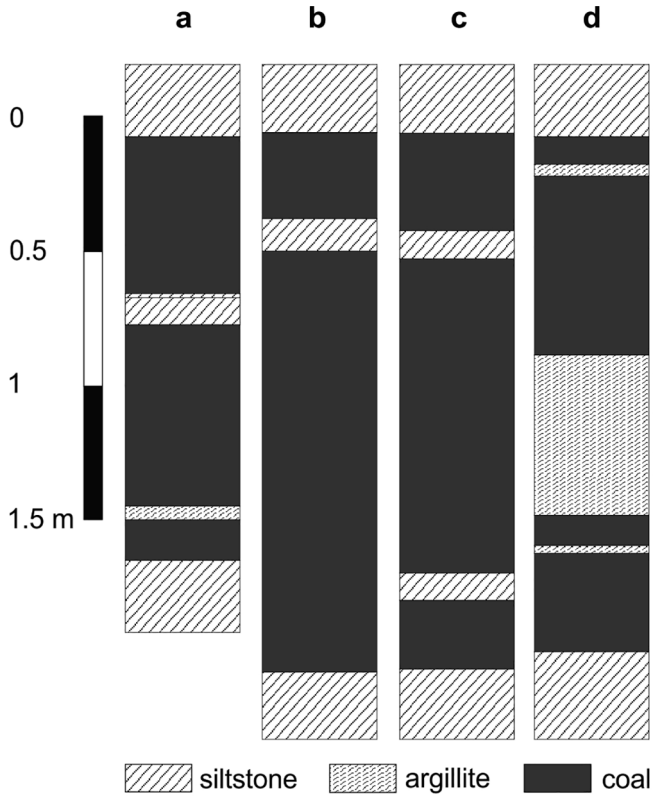

Fig. 4. Structure of the seam XI. a – Raspadsky open cut; b – Shevyakov mine; c – Lenin mine; d – Tomusinsky open cut.

3. Results

3.1. Structure and petrographic composition of seam XI

The seam has a rather uneven thickness, but it stretches over considerable distances with the thickness ranging from 0.3 to 5 m. The average thickness decreases from east to west. In the west of the basin, seam XI lenses out and has no commercial significance.

The seam structure is rather stable. Usually, it is represented by two coal bands separated usually by a non-coal interlayer of 6 to 15 cm and rarely more (Fig. 4). In some areas, one or two thinner (1–4 cm) interlayers of argillite appear in the lower band.

The coal in the seam section is characterized by variable ash yield ranging from low (< 10%) to high. (> 40%) In general, the coal has low phosphorous (P_2O_5 < 0.02%) and low sulfur (S_t < 0.6%). The maceral composition of the studied sections is dominated by vitrinite (42.2%) with lesser amounts of semivitrinite (6.9%) (Table 1). The inertinite content is also rather high, with an average of 33.1%.

The ratio of vitrinite and inertinite macerals varies significantly, pointing to unstable conditions of paleo-peat accumulation. There was a periodic drainage of the swamp resulting in the inertinite content increasing. The sum of the oxidizing components in the coals ranges from 18 to 70%. The coals directly below and above the intrastratal rock interlayer have similar characteristics in terms of the basic macerals content and the sum of the fusenite components. This fact indicates that the accumulation of the rock interlayer had no effect on the geodynamic situation within the basin. This feature seems to reflect an irregular, catastrophic nature of the rock interlayer accumulation in the coal seam, possibly caused by aeolian fallout of mineral matter from a remote source. This is partially confirmed by significant areas of this horizon distribution at a relatively little, but rather moderate thickness of 6 to 15 cm, and rarely thinner. In the open cuts and underground mines the upper interlayer is recognized by the increased radioactivity of 30–50 μR/hour, significantly exceeding the radioactivity of coal-

Table 1
Maceral composition, ash yield, and reflectivity of vitrinite of the coal seam XI (Raspadsky cut).

Sample number	Interval thickness, cm	Macerals, %			ΣOC	Wa,%	A^d, %	$R_{o,n}$
		Vt	*Sv*	*I*				
PK-2–18	5.0	28	7	32	37	0.66	28.5	1.532
PK-3–18	5.0	41	7	36	41	0.46	9.9	1.482
PK-4–18	5.0	25	8	48	53	0.40	15.4	1.482
PK-5–18	5.0	38	6	45	49	0.31	6.9	1.477
PK-6–18	5.0	16	5	38	41	0.44	12.3	1.460
PK-7–18	5.0	47	6	29	33	0.39	8.7	1.488
PK-8–18	5.0	12	10	51	58	0.36	18.7	nd
PK-9–18	5.0	33	7	22	27	0.33	10.5	1.500
PK-10–18	5.0	7	8	65	70	0.35	19.4	nd
PK-11–18	5.0	45	11	29	36	0.36	8.3	1.491
PK-12–18	5.0	44	6	35	39	0.30	9.9	1.502
PK-13–18	3.0	48	6	28	32	0.30	13.1	1.490
PK-14–18	1.5	nd	nd	nd	nd	0.86	71.9	nd
PK-15–18	10.0	nd	nd	nd	nd	1.20	87.8	nd
PK-16–18	2.0	16	9	22	28	0.49	46.4	nd
PK-17–18	5.0	46	7	24	29	0.37	17.0	nd
PK-18–18	3.0	37	5	35	38	0.32	14.3	1.487
PK-19–18	3.0	43	6	34	38	0.28	13.4	1.494
PK-20–18	5.0	35	6	23	27	0.33	9.4	1.496
PK-21–18	5.0	35	13	40	49	0.38	10.9	1.504
PK-22–18	5.0	14	10	33	40	0.36	17.8	nd
PK-23–18	5.0	15	6	39	43	0.42	13.9	1.491
PK-24–18	5.0	40	6	26	30	0.50	8.3	1.490
PK-25–18	5.0	41	7	27	32	0.36	5.4	1.509
PK-26–18	8.0	39	5	21	24	0.36	5.4	1.497
PK-27–18	5.0	50	5	15	18	0.36	3.5	1.487
PK-28–18	5.0	28	6	23	27	0.34	5.2	1.487
PK-29–18	5.0	48	3	30	32	0.36	5.0	1.494
PK-30–18	5.0	50	9	30	36	0.34	3.7	1.502
PK-31–18	2.0	17	1	10	11	0.73	67.1	nd
PK-32–18	5,0	47	5	37	40	0.36	5.0	1.486
PK-33–18	10,0	10	nd	8	8	0.52	57.2	nd
Mean		35.3	6.9	33.1	37.8	0.39	11.4	1.493

Note: nd – no data available; Vt – vitrinite, Sv – semivitrinite, I – inertinite, ΣOC – sum of fuseniting components, Wa – moisture content, A^d – ash yield for dry matter, $R_{o,n}$ – reflectivity of vitrinite in oil immersion.

bearing rocks. Due to the presence of the rock interlayer with the increased radioactivity, the seam XI is easily identified by gamma-ray logging.

3.2. Chemical composition of the coal, coal ash and rock interlayer in seam XI

The mean concentrations of trace elements in the coal, coal ash, and in the interlayer of the seam XI are shown in Table 2. According to these data, the coal and especially the coal ash, are characterized by abnormally high concentrations of Nb, Ta, Zr, Hf, Ag, Be, Sn, Y, and REE, as well as higher concentrations of Li, Ga, Co, Ni, Cu, Ba, Mo, W, Pb, and Th compared to the mean concentrations in coals of the world (Ketris and Yudovich, 2009). In specific intervals their concentrations can reach significant values. Thus, Zr concentrations directly above the rock interlayer reach 1.39%, and Nb is up to 0.43%. Many lithophilic elements are anomalous near the rock interlayer and directly in it. Yttrium concentration reaches 286 ppm, Hf – 173 ppm, Sn – 31 ppm, Ga – 81 ppm, Be – 109 ppm, sum of REE – 0,19%, Th – 97,8 ppm, U – 59,4 ppm, W – 43 ppm, and Ta – 71 ppm. All these anomalies are clearly confined to the thin rock horizon (interlayer). The interlayer is distinguished by increased radioactivity (30–50 μR/h) and abnormal concentrations of a large group of rare metals, including Zr, Nb, Ta, Hf, Y, REE, Sn, Th, and U (Table 2).

Concentrations of some other elements are also anomalous in the coal ash. Thus, in different sections of the seam, Cu concentrations in some coal ash samples exceeds 400 ppm, Zn concentrations exceeds 400 ppm, and Pb concentrations exceeds 196 ppm.

All these data together allow us to identify a specific Nb(Ta)-Zr(Hf)-REE(Y) mineralization in the seam XI with a group of associated metals (Ga, Li, Sn, and others). Ores of such a composition were identified and studied in detail in China (Dai et al., 2010, 2012b). However, the mineralization in seam XI has its own specific characters, based on both the element concentrations and the nature of the interlayer which is considered the source of the mineralization.

3.3. Nb and Ta

The Nb and Ta accumulation levels in seam XI are the most significant. The mean Nb concentration for the coal ash is 650 ppm, which is 32.5-times higher than the average for coal ash of the world (Ketris and Yudovich, 2009). The mean weighted concentration for the coal ash including the rock interlayer is slightly lower – 482 ppm. Expressed as oxides (Nb_2O_5) this is 930 and 689 ppm. The Nb concentration in the rock interlayer is 264 ppm, which is 10.6 times higher than the average for the Earth's crust (Taylor and McLennan, 1985).

The Nb distribution in the seam section is very irregular. We can see that the highest concentrations are clearly related to the rock interlayer (Fig. 5), suggesting a genetic link. At the same time, the levels of Nb accumulation in the coal ash above the tonstein are higher than under it. The enrichment zone above the interlayer has higher values, but is thinner, whereas the zone below has lower values but is thicker. The Nb concentration in the ash ranges there from 0.43 to 0.13%. Mean concentrations, and especially local Nb concentrations in the coal ash, significantly exceed those described in coal-bearing sediments in China and other regions of the world (Seredin, 2004; Seredin and Finkelman, 2008; Dai et al., 2010, 2012b, 2014).

A unique feature of the rock interlayer is a high Ta concentration of 42 ppm on average for 12 sections with a range from 28 to 71 ppm. Higher local concentrations, up to 220 ppm, have been recorded in only one coal deposit in the world (Bouška and Pešek, 1999). Such concentrations (up to 270 ppm) were also found in the north of Kuzbass in the coal ash of the seams Gorely, Volkovsky, and Podvolkovsky I (Nifantov et al., 2014). They are age analogs of the seam XI. The Nb/Ta ratio varies from 4 to 6 in the rock interlayer and from 79 to 144 in the coal ash of the lower and upper coal bands, respectively. This indicates a significantly higher mobility of Nb compared to Ta in the process of the interlayer alteration with Nb loss and formation of the rare-metal mineralization in the near-contact zone. Tantalum concentration in the coal ash in the lower band is 10 ppm, and in the upper band it is only 3.2 ppm with abnormally high Nb concentration (Table 2). Such features of Nb and Ta distribution and Nb/Ta ratio in a coal seam section were described for late Permian coals from Huayingshan Coalfield, Sichuan, southwestern China (Dai et al., 2014).

3.4. Zr and Hf

The mean Zr concentration in the coal seam XI is 213 ppm, in the coal ash it is 1870 ppm and in the coal ash with the rock interlayer it is 1751 ppm (Table 2). In terms of oxides this is 2256 and 2365 ppm, respectively. The Zr accumulation coefficient in the coal ash of the seam XI in relation to the mean value for coals of the world is 8.9 (Ketris and Yudovich, 2009). The interlayer contains 1910 ppm of Zr, which is also 10-times higher than the mean concentration for the upper continental crust (Taylor and McLennan, 1985).

Zirconium is characterized by the same type of distribution in the seam section as Nb. The highest Zr concentrations in the coal ash were observed directly above the rock interlayer, where they reach up to 1.39%. The zone of the coal enrichment in the upper band above the interlayer is relatively thin, whereas in the lower band, the enrichment zone it is much thicker, but concentrations are not so high (Fig. 6).

This type of Zr distribution in the vicinity of altered volcanogenic pyroclastics (tonsteins) has long been identified and described for

Table 2
Trace element concentrations in the coals, coal ash and rock interlayer in the seam XI (ppm) from the Raspadsky cut.

Elements	Upper band (PK-1–18)		Rock[1] interlayer (PK-15–18)	Lower band (PK-34–18)		The entire seam			Mean concentration in the world[3]		CC[4]
	coal	ash		Coal	ash	coal	ash	ash[2]	coal	ash	
Li	34.0	239	43.2	12.7	128	21.9	186	136	12	66	2.8
Be	5.9	41.5	14.6	2.9	29.3	4.2	36.6	26.4	1.6	9.4	3.9
Sc	2.4	16.9	7.8	0.92	9.3	1.6	13.7	10.4	3.9	23.0	0.6
V	17.6	123.9	49.6	7.2	72.7	11.7	103	78.0	25.0	155	0.7
Cr	15.0	106	79.6	8.4	84.8	11.2	98.5	86.2	16.0	100	1.0
Co	18.5	130	12.1	8.6	86.9	12.9	113	68.6	5.1	32.0	3.5
Ni	27.7	195	25.5	24.9	252	26.1	229	140	13.0	76.0	3.0
Cu	19.0	134	60.5	10.7	108	14.3	126	97.2	16.0	92.0	1.4
Zn	16.3	115	291	11.9	120	13.8	121	176	23.0	140	0.9
Ga	5.3	37.3	80.6	3.2	32.3	4.1	36.1	51.6	5.8	33.0	1.1
Ge	0.9	6.2	3.4	0.9	8.9	0.9	7.5	6.0	2.2	15.0	0.5
As	1.6	11.4	6.0	3.8	38.2	2.8	24.2	16.8	8.3	47	0.5
Se	1.1	7.7	6.8	0.8	7.7	0.9	7.7	7.5	1.3	8.8	0.9
Br	1.5	10.7	0.83	0.8	7.9	1.1	9.7	5.8	5.2	32	0.3
Rb	6.0	42.2	62.8	2.6	26.3	4.1	35.8	44.5	14.0	79	0.5
Sr	28.8	203	205	94.0	949	65.8	578	417	110	740	0.8
Y	20.7	146	118	15.0	152	17.4	153	129	8.4	51.0	3.0
Zr	207	1457	1910	217	2191	213	1870	1751	36.0	210	8.9
Nb	65.5	461	264	78.5	793	72.9	650	482	3.7	20	32.5
Mo	4.9	34.4	0.7	2.3	23.7	3.5	30.3	17.8	2.2	14.0	2.2
Ag	0.39	2.8	2.8	0.38	3.8	0.38	3.4	3.1	0.095	0.61	5.6
Cd	0.18	1.3	2.6	0.16	1.6	0.17	1.5	1.8	0.22	1.2	1.3
Sn	1.0	7.0	35.0	1.2	11.7	1.1	9.4	17.6	1.1	6.4	1.5
Sb	1.0	6.9	1.3	0.6	6.1	0.76	6.7	4.4	0.92	6.3	1.1
Te	0.017	0.12	0.2	0.020	0.20	0.018	0.16	0.17	nd	nd	
Cs	0.30	2.1	4.0	0.17	1.7	0.22	2.0	2.7	1.0	6.6	0.3
Ba	157	1105	565	151	1525	154	1348	1006	150	940	1.4
La	12.1	85.2	149	19.1	193	16.1	141	140	11	69.0	2.0
Ce	23.6	166	302	36.6	370	31.0	272	277	23	130	2.1
Pr	2.7	19.0	32.5	4.1	41.4	3.5	30.9	30.7	3.5	20.0	1.5
Nd	9.7	68.3	107	14.1	142	12.2	107	104	12.0	67.0	1.6
Sm	2.3	15.9	24.0	3.0	30.3	2.7	23.5	22.5	2.0	13.0	1.8
Eu	0.29	2.0	1.6	0.26	2.6	0.27	2.4	2.0	0.47	2.5	1.0
Gd	2.7	18.7	26.0	2.92	29.5	2.8	24.7	23.6	2.7	16.0	1.5
Tb	0.47	3.3	4.5	0.46	4.6	0.46	4.1	3.9	0.32	2.1	2.0
Dy	3.1	21.5	24.2	2.6	26.0	2.8	24.4	22.5	2.1	14.0	1.7
Ho	0.71	5.0	4.5	0.54	5.5	0.61	5.4	4.7	0.54	4.0	1.4
Er	2.16	15.2	12.2	1.56	15.8	1.82	16.0	13.5	0.93	5.5	2.9
Tm	0.31	2.2	1.8	0.22	2.2	0.26	2.3	1.9	0.31	2.0	1.2
Yb	1.82	12.8	9.7	1.34	13.5	1.55	13.6	11.0	1.0	6.2	2.2
Lu	0.28	2.0	1.5	0.19	1.9	0.23	2.0	1.7	0.20	1.2	1.7
Hf	3.4	23.7	76.4	4.1	41.3	3.6	31.8	42.1	1.2	8.3	3.8
Ta	0.45	3.2	56.4	0.99	10.0	0.79	6.9	22.0	0.28	1.7	4.1
W	2.1	14.6	2.7	0.87	8.8	1.4	12.2	8.2	1.1	6.9	1.8
Re[5]	< 1	< 7	< 1	1.5	16	1.0	8.0	4.6	nd	nd	
Au	< 0.002	< 0.01	< 0.002	< 0.002	< 0.01	< 0.002	< 0.01	< 0.01	0.0037	0.022	
Hg[5]	12	84.5	763	17	172	15	127	379	100	750	0.2
Tl	0.052	0.36	0.76	0.054	0.55	0.053	0.47	0.62	0.63	4.9	0.1
Pb	11.3	79.6	39.8	7.4	75.1	9.1	79.9	62.0	7.8	47.0	1.7
Th	4.5	31.7	80.7	3.9	39.5	2.9	25.6	32.4	3.3	21.0	1.2
U	1.72	12.1	15.9	1.70	17.2	1.6	13.6	14.3	2.4	16.0	0.9
ΣREE	62.1	437	700	87.1	880	76	670	660	60.1	353	1.9

Note: nd – no data available; 1 – volcanogenic (rock) interlayer; 2 – in the coal ash with the rock interlayer included; 3 – mean concentrations for coals (Ketris and Yudovich, 2009); 4 – CC ratio of the mean concentration in the coal ash to the mean concentration for the ash of coals of the world; 5 – ppb; Concentrations of Hg, Tl, Re, Li, As, Sb, and Br in the coal ash were recalculated from their concentrations in the coal.

several regions (Crowley et al, 1989, Hower et al., 1999; Arbuzov et al., 2000; Arbuzov et al., 2016; Vergunov et al, 2019).

The Hf concentrations are also abnormal, with an average of 31.8 ppm in the coal ash and 42.1 ppm in the ash includng the rock interlayer (Table 2). The accumulation coefficient in relation to the mean concentration in coals of the world is 3.8 (Ketris and Yudovich, 2009). The interlayer contains 76.4 ppm of Hf on average, which is 13.2-times higher than the mean for the upper continental crust (Taylor and McLennan, 1985).

The Hf distribution in the section is comparable to that of Zr, which is not surprising given the geochemical affinity of these elements. However, the Zr/Hf ratio in the coal ash near the rock interlayer (60–80) is much higher than in the interlayer (30) and in the coal ashes at a distance from it (30–40). This points to lower Hf mobility during alteration compared to Zr.

3.5. Rare-earth elements (lanthanides and yttrium).

From the group of rare-earth elements, significant accumulation was only found for the lanthanides. The coal, coal ash and rock interlayer are not enriched in Sc. Maximum local Sc concentrations in the coal ash do not exceed 28.8 ppm.

The mean concentration of the REE sum in the coal seam XI is 93.4 ppm, in the coal ash it is 823 ppm and in the coal ash with the interlayer it is 788 ppm (Table 2). In terms of oxides this is 975 and 934 ppm. These values are not particularly high, but they are two-times

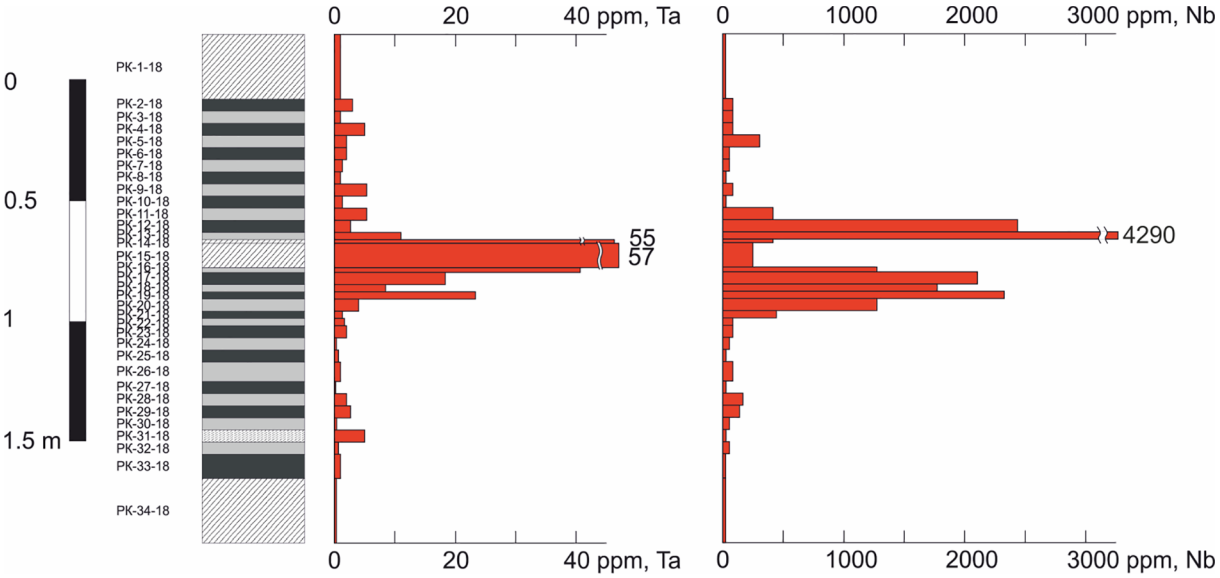

Fig.5. Distribution of Nb and Ta in the seam XI section. A – Raspadsky open cut, B – Shevyakov mine, C - Lenin mine.

higher than the mean concentrations of the coals of the world (for coal ash) (Ketris and Yudovich, 2009).

The REE distribution in the coal section is not as clearly connected with the rock interlayer as is the case for Nb and Zr. This may be due to the greater mobility of REE in water during early diagenesis. The seam area directly under the interlayer is distinctly enriched. It affects the difference in REE concentration in the upper and lower bands with the lower band containing 880 ppm of REE sum in the coal ash and the upper band containing only 437 ppm. As noted by Hower et al (2016), observed concentrations of REE and the relative distributions of the lanthanide elements are the sum of the entire geologic history of the coal.

Following the recommendations of Seredin and Dai (2012), for preliminary estimation of the conditions of lanthanides accumulation in the coals, ratio calculations of the REE concentration in the coal to the mean in the Earth crust were made. Seredin (2001) distinguished four main types of the REE distribution in coals: N, L, M, and H. The letters N, L, M, and H mark different graph types obtained by the ratioing REE concentrations in samples to the mean concentration in the coals of the USA or North American shale composite (NASC). N is a normal type for the earth's crust (REE spectra are parallel to the NASC spectra). L, M, and H types are characteristic of the relative accumulation of the light (LREE), mean (MREE), and heavy (HREE) rare-earth elements (Seredin, 2001). Later the methods were modified by way of normalization of the element contents in coals to their Clarke value in the upper continental earth's crust (Seredin and Dai, 2012). This classification is widely used at present as it makes it possible to estimate, to a first approximation, the nature of the lanthanide accumulation in coals. We suggest that the REE in coals with N and L types of distribution originate from the input of detrital sediment material and the REE in coals with the M and H type distribution originate from water solutions.

The graphs normalized to the mean in the upper continental crust (after Taylor and McLennan, 1985) show that the upper band follows the H-type of graph, indicating the predominant accumulation of REE due to hydrogenesis (Fig. 7A). At the same time, the Eu anomaly is clearly shown, indicating the predominant influence of felsic rocks on the REE accumulation in the coals of this band.

The negative Eu anomaly is present in the lower parts of the, but the

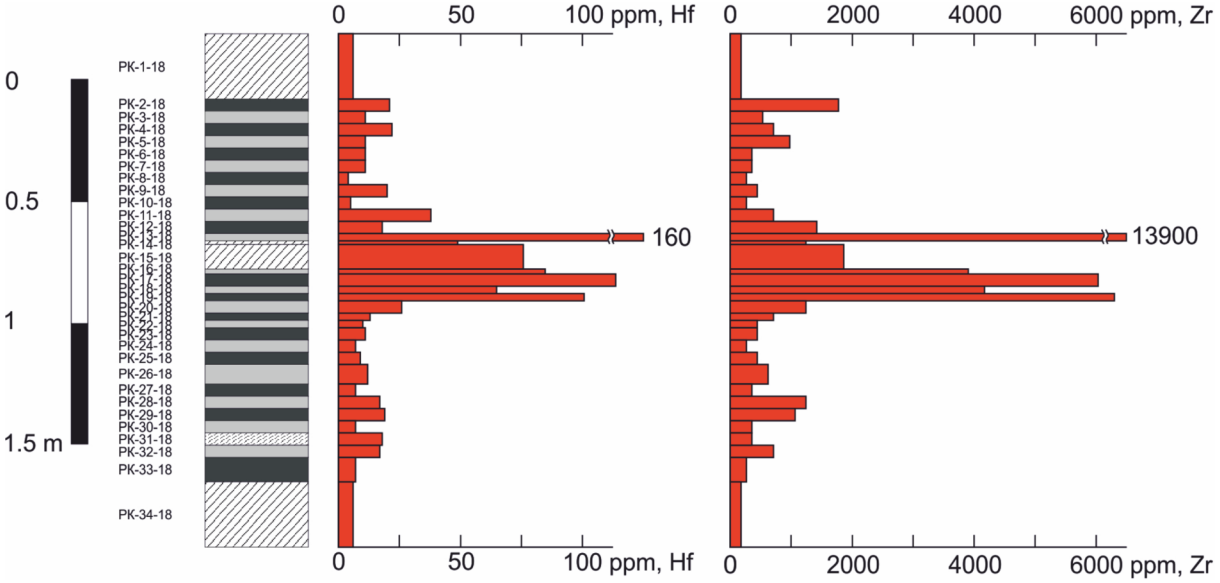

Fig. 6. Zr and Hf distribution in the seam XI.

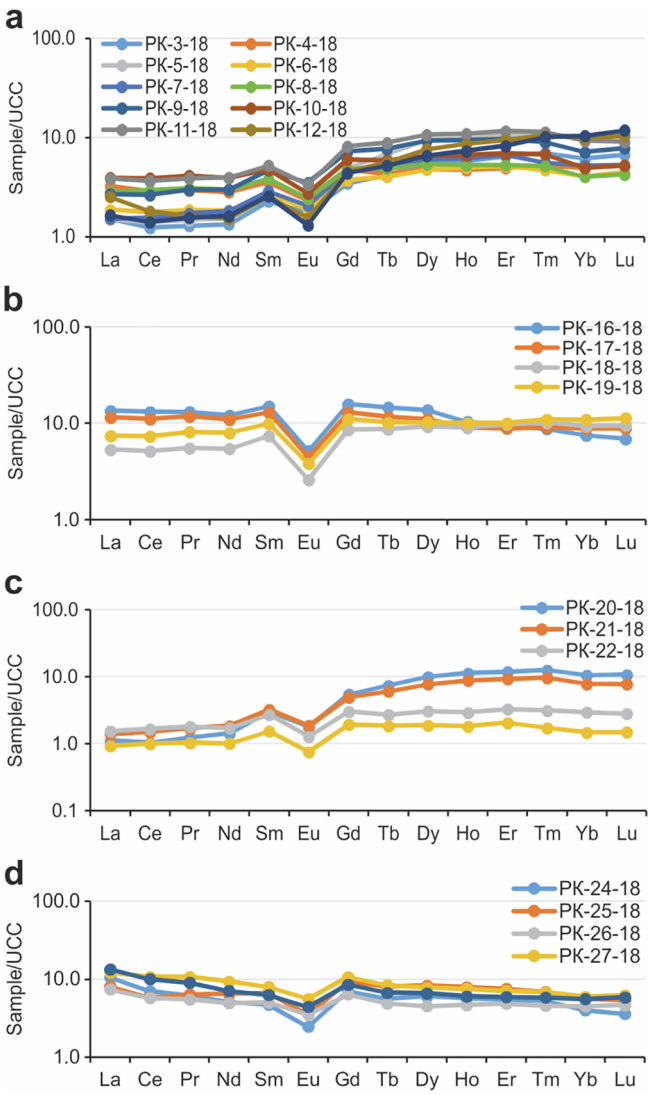

Fig. 7. Normalized graphs of REE distribution in the coal ash in the seam XI (Kuzbass). A – coal of the upper band of the seam XI; B - coal under the rock interlayer; C – middle part of the coal band; D – lower part of the coal band. Calculations were made to the mean in the upper continental crust (Taylor, McLennan, 1985).

size gradually decreases with distance from the interlayer to the bottom of the seam (Fig. 7 B, C, D). The L-M-type of the normalized curve (Fig. 7 B) is distinct in the lower band directly under the interlayer, which gradually transforms into H-type (Fig. 7 C), and then again into L-type (Fig. 7D). The transition occurs gradually as a consequence of the geochemical zoning due to different mobilities of light and heavy REE in water solutions. The differing distributions indicate the importance of element redistribution both at the peat accumulation stage and during the subsequent coal transformation.

3.6. Ga

Although Ga does not determine the economic importance of the rare-metal mineralization of the layer XI, it is an important co-element having concentrations comparable to those of commercial significance (Seredin, 2004; Seredin and Dai, 2012; Dai et al., 2012b; Dai and Finkelman, 2018). In the coal and coal ash, Ga concentrations are normal and are comparable to the mean values for coals of the world. However, in the rock interlayer it reaches up to 80 ppm. Gallium slightly migrates in the process of pyroclastic alteration. As a consequence it enriches coals only in direct contact with the interlayer. Its average concentration in the coal ash in the seam is 51.6 ppm (Table 2). According to this characteristic, Ga is close to Ta, forming a single association. Their concentrations are strongly anomalous in the rock interlayer and a little higher in the coal ash of the seam XI.

3.7. Radioactive elements (U and Th)

Concentrations of radioactive elements in the coal seam XI are far from being of commercial importance, but they are important as indicators of this type of mineralization in coal. They enable these horizons to be detected, which are responsible for the formation of this type of rare-metal mineralization. Due to their high radioactivity (30–50 μR/h), they are easily detected by gamma-ray logging or by small-size radiometric equipment directly in mines. The mean uranium and thorium concentrations in the coal ash of the seam XI are 14.3 ppm and 25.6 ppm, respectively. These values are comparable with the mean in coals of the world (Table 2). At the same time, the rock interlayer contains 15.9 ppm of U and 80.7 ppm of Th. In coal ash at the contact with the rock interlayer the Th concentration reaches 97.8 ppm and U concentration reaches 59.4 ppm. Their distribution in the section is close to the distribution of other elements specific for this mineralization. The high correlation coefficient between U and Th in the coal (0.92) and coal ash (0.84) indicates their joint migration and points to a reducing environment. Under oxidizing conditions, the formation of the more soluble uranyl ion would enable U to migrate more readily, thus breaking the correlation (Titaeva, 2005).

3.8. Mineral composition

The geochemical studies shown that the complex Nb-Ta-Zr-Hf-Y-REE-Ga element association found in seam XI is closely related to the rock interlayer dividing the seam into two bands. The concentrations of essential valuable elements clearly decrease with distance from the interlayer. The interlayer itself is also anomalous in terms of the concentrations of these elements. In particular, Ta concentration reaches 71 ppm, which is considered a commercial mineralization (Yegyan and Rozhanets, 2008). In this regard, the mineral composition of the rock interlayer is of particular interest.

The study of the petrographic composition of the rock interlayer using the optical microscope shows that it is a clastic rock of siltstone dimensions (Fig. 8A). The extreme angular character of the fragments is visible under the electron microscope. Tabular and prismatic feldspar crystals set in a clay matrix are clearly visible (Fig. 8B). In some sections, there is up to 5% siderite. Kaolinite, hydromica, and siderite are of secondary origin and often form pseudomorphs on the primary minerals or occur in veins (Fig. 8C). The interlayer contains numerous crystalloclasts of quartz and feldspars. Small volcanic clasts, possibly of rhyolite initially, replaced by kaolinite are common (Fig. 8D). Clasts with a lapilli structure are also observed. (Fig. 8E). Grains are not orientated nor is stratification visible in the interlayer. The grains of feldspar, and especially quartz, are often elongate, angular and are randomly orientated. (Fig. 8F).

Lack of evidence of water transportation, based on lack of sorting and stratification, strongly suggests aeolian transportation and a one-act sedimentation of the clastic material. The predominance of clay-hydromica material with a large fraction of porphyroclasts in the rock suggests alteration of a significant part of the unstable primary sediments in diagenesis and early catagenesis. The most likely precursor of clay-hydromica material would have been volcanic glass, which is not stable in the peat environment. It is possible that fine-grained glass was originally present in the form of accretionary lapilli.

The X-ray analysis of several sections of the interlayer demonstrates the predominance of quartz (37.2%), albite (13.9%), potassium feldspar (6.2%), relic mica minerals (8.6%), and newly formed minerals of the smectite group (15%) and kaolinite group (7.9%). Small amounts of

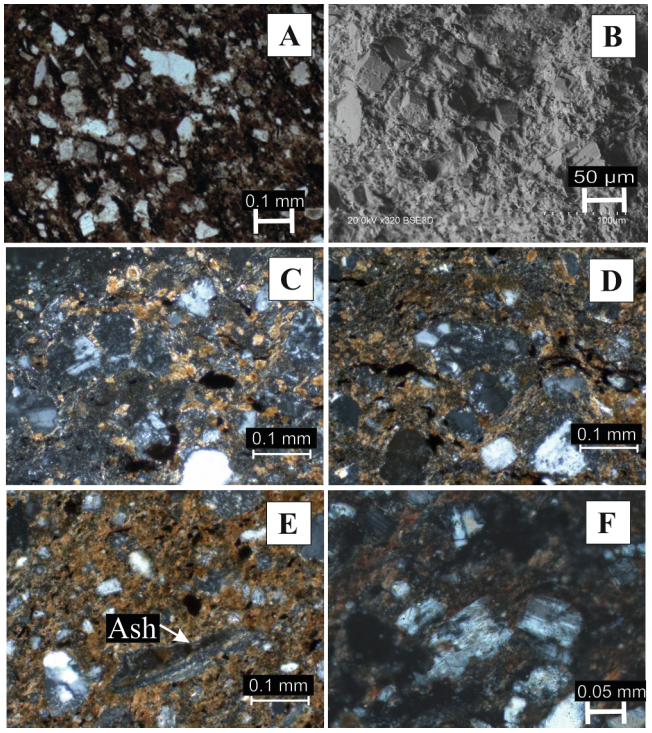

Fig. 8. Rock structure of the interlayer in the seam XI. 8 A, C, D, E, F – thin section. Optical microscope. B – Fracture image in backscattered electrons. A – structure of the rock interlayer in the seam XI; B - Tabular and prismatic feldspar crystals; C – development of the hydromica and siderite; D – rhyolite clast (in the center). The essential mass is replaced by kaolinite. Fine unreplaced relic crystals can be seen; E – Relic clast of volcanic ash, replaced by kaolinite; F – corroded tabular crystal clasts of chess-board albite.

Table 3
Mineral composition of the rock interlayer in the seam XI, %

Mineral	Content,%	
Quartz	37.2	44.6
Kaolinite	7.9	6.5
Albite	13.9	17.4
Christobalite	1.1	0.5
Sodalite	2.1	2.7
Tridymite	0.9	1.2
Anatase	1.1	1.0
Gypsum	0.6	0.5
Smectite, ML*	15.0	12.2
Illite	8.6	7.8
Feldspar (sanidine)	6.2	5.6
Siderite	4.3	–
Chloroapatite	1.1	–
Total	100.0	100.0

Note: ML – mixed-layer clay mineral.

siderite (4.2%), sodalite (2.1%), anatase (1.1%), crystobalite, and tridimite are present (Table 3) in the rock.

K-feldspar is predominantly represented by sanidine. Albite is represented by tabular short prismatic shapes with polysynthetic counterparts. Fine phenocrysts of chess-board albite are well defined in the thin sections due to their specific double lattice (Fig. 8F). Mica minerals are generally represented by hydromica (illite). Besides the hydromica, there are relic crystals (laths) of strongly replaced brown biotite. In these laths the K, Mg and Fe concentrations are not more than 2%.

Numerous albite, kaolinite, and mixed-layer crystals of iron-magnesium chlorite (chamosite) and illite were found in the rock interlayer. Specific globular and nodular forms of illite and mixed-layer formations were found (Fig. 9). It is possible that these represent original accretionary lapilli now replaced by clay minerals. The shape of albite crystals is prismatic, lamellar, and, in some cases, there are signs of corrosion.

At the boundary above and below the rock interlayer, a significant number of newly formed quartz and albite aggregates were observed in the coals. Globular, nodular, and tabular forms of quartz are abundant (Fig. 10). These forms are largely due to the fact that quartz partially or completely fills pore spaces which have both an ovoid and a less regular elongate shape. Concentrations of quartz globules are often formed in cracks in coal. There is no doubt that they have a secondary nature in relation to the rock interlayer and coal. Probably, the silica was partially leached from the rock and re-deposited into the coal.

3.9. Zr and Nb

Zirconium minerals are represented by zircon, complex Nb-Zr silicates, and Fe-Ti-Nb-Zr oxides. The zircon crystal sizes rarely reach up to 30 µm (Fig. 11A). All grains have up to 2% Hf impurities. There are extremely rare, larger crystals. In the less-altered central part of the interlayer, Zr mineralization is represented mainly by micro-inclusions of zircons in mica laths (Fig. 11E). The primary mica is strongly altered with the formation of hydromica with low concentrations of K (of about 2%), Mg, and Fe. The initial composition probably corresponded to biotite.

Newly formed minerals of zirconium and niobium are represented by a group of Ti-Nb-Zr oxides with a variable amount of Ti, Nb, Zr, and Fe (Fig. 11 B, C, D). Earthy aggregates of Ti oxide with admixture of Zr and Nb are also found (Fig. 12).

In coals above and below the rock interlayer, Nb and Zr are present in Zr-Nb-Fe-Ti oxides with a variable amount of each element. This phase is diagnosed by X-ray phase analysis as rutile or anatase. Zirconium is also present in zircon. Zircons have been identified as both small and well-bounded zircons and large relict ones with some corrosion. Fine zircons were mainly found in aluminosilicate veins, but also in large aluminosilicate aggregates. The crystal sizes are about 1.5 µm and less (Fig. 13). In addition there are rare, much larger grains of zircon without inclusions, which show signs of corrosion and are thought to be relict.

Zircons are known to be relatively stable in the hypergenesis zone. They are also resistant to various mineral acids. However, metamict varieties (malacone, cyrtolite) are easily decomposed. The low content of zircon in the volcanogenic interlayer accompanied by high concentrations of zirconium may be associated with the destruction of U-Th-enriched metamict zircons and the formation of Zr-Nb-Ti-Fe oxides. Uranium and thorium are included in newly formed minerals. The possibility of such a model is indicated by the anomalous radioactivity of the volcanogenic interlayer and significant enrichment of uranium and thorium in the coal in the contact zone.

3.10. Rare-earth elements (REE)

In the rock interlayer, REE are mainly represented by neodymium fluorine-carbonate, or bastnaesite (Fig. 14). It is found both in the basic mass in the form of irregular segregations and in the pores of altered primary minerals, such as albite (Fig. 14B), that indicates its secondary, diagenetic, or epigenetic nature.

In the coals both below and above the rock interlayer, REE are in fluorocarbonates (bastnesite) and phosphates (monazite, xenotime) (Fig. 15). As a rule, monazite and xenotime are found in the form of micro-aggregates, but it is impossible to distinguish between them because of the extremely small (nanometer) size of separate grains. In addition there are mixed aggregates of monazite and fluorocarbonate (Fig. 15C,D).

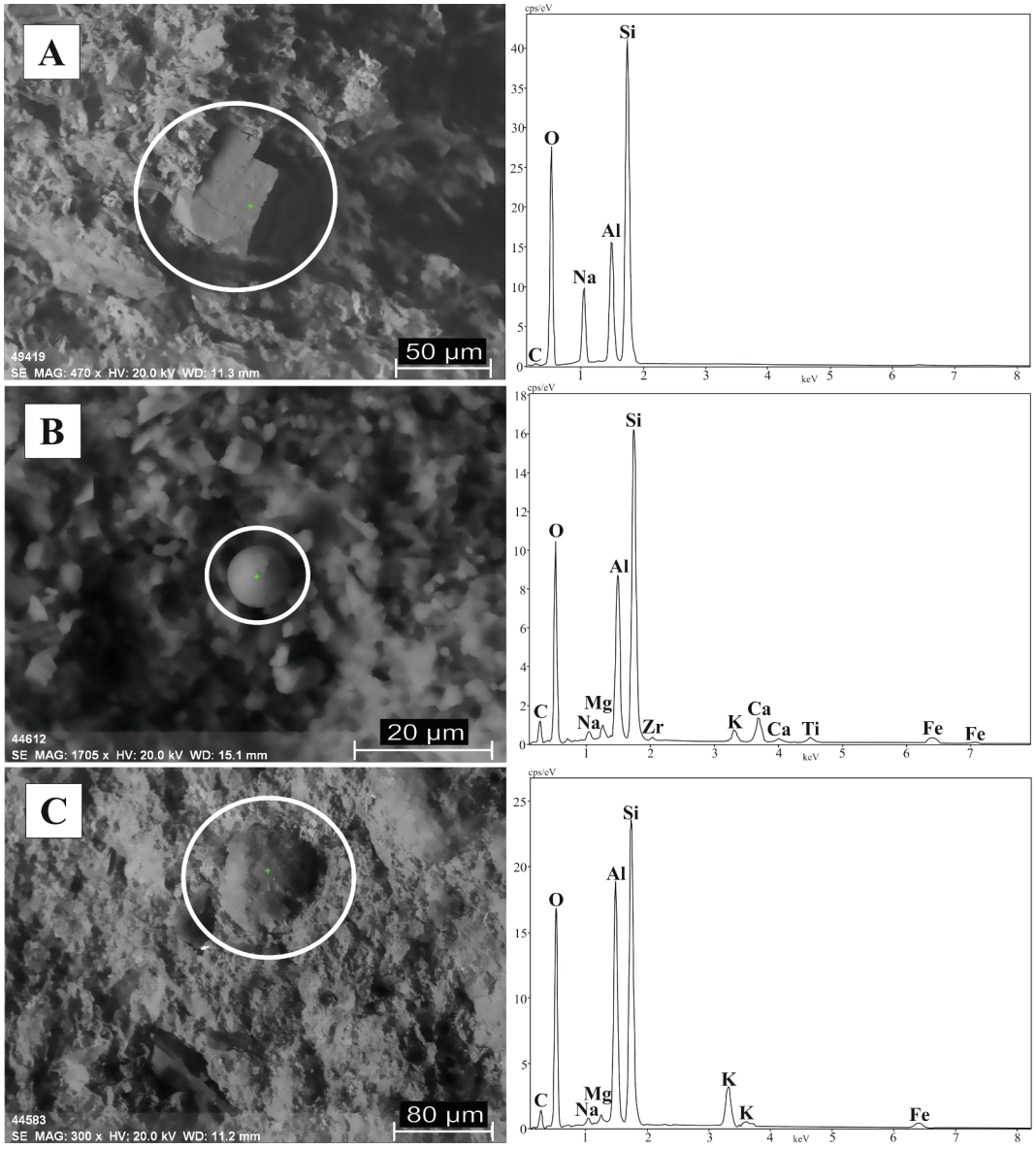

Fig. 9. Prismatic albite crystal (A), globular mineral particles of smectite group (B) and nodular illite particles (C).

3.11. Other mineral phases

Sulfides (pyrite, sphalerite, galena, molybdenite, and chalcopyrite), native metals, and intermetallic compounds were found in the rock interlayer. Sphalerite is the most common. Barite, a sulfate was also found. Among native and intermetallic compounds are Au, Cu-Zn, Zn, Ni(Cu,S), Pb-Cu-Zn (Fe), W, and W-Co.

At the contact with the rock interlayer, sulfides mainly fill the pores and the space in the cell tissue of fusenites. Almost all sulfides in the pores have a characteristic nodular form, whereas in fusenite cells the sulfides form elongate-cylindrical particles.

4. Discussion

4.1. Nb(Ta)-Zr(Hf)-REE-Ga mineralization origin in the coals

As the above data demonstrated, the complex Nb(Ta)-Zr(Hf)-REE-Ga association of the seam XI of the Kuznetsk Basin are distinctly spatially and genetically related to the intra-coal rock interlayer. This is evidenced by the character of the distribution of these elements in the seam and by peculiarities of the mineral and chemical composition of the ores and the interlayer.

The diagrams of REE distribution in the coals of seam XI, in the non-coal interlayer and in the enclosing rocks, normalized to the mean concentration of the upper continental crust, differ significantly. The presence of a contrasting negative Eu anomaly (Fig. 7) makes it possible to identify a direct connection between the REE accumulation in coals and the rock interlayer and, at the same time, demonstrate that both are linked to felsic rocks. The absence of this anomaly is associated with the overlying roof and underlying floor rocks, which have a typical REE pattern for terrigenous sediments (Fig. 16).

The correlation analysis shows that Zr and Nb concentrations in the coal have no significant correlation with the ash yield and in the coal ash it is generally negative. This indicates different sources of these metals in the coal other than the detrital material. It also follows that Zr and Nb accumulation in the coal at the contact with the rock interlayer could not occur due to the input of terrigenous-clastogenic material but due to water solutions. The migration capacity of this group of elements in the fresh waters of the hypergenesis zone is low, thus limiting the possibility of their accumulation in the coal due to the hypergenesis zone waters during the peat accumulation or early diagenesis. The inflow of these elements into the coal-bearing sediments under natural

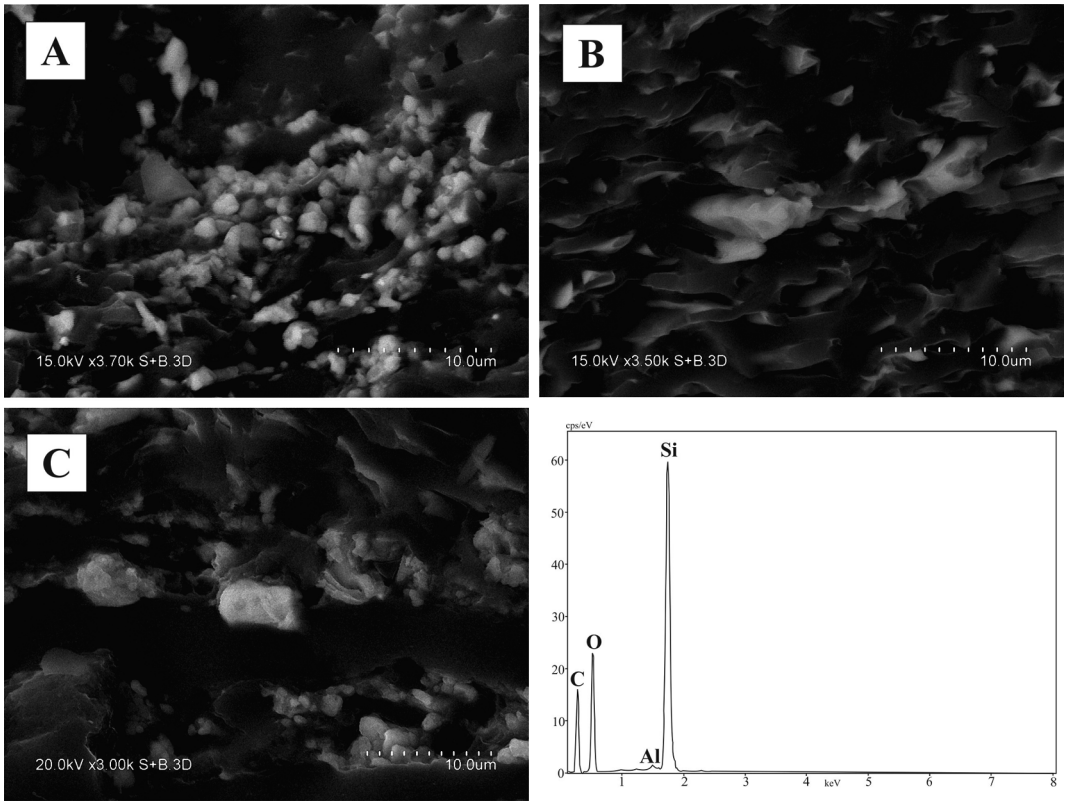

Fig. 10. Globular (A) and lamellar (B) quartz particles. C – nodular quartz formations in coal pores. In the center it is a prismatic crystal of chalcopyrite.

conditions is possible due to sulfurous water (Vakh et al., 2013). However, abundant sulfates should have formed in the coal, as well as sulfides as a result of the sulfate reduction, which is not observed in this case. The coal of seam XI is poor in sulfur (< 0.6%) and the sulfide content in them does not differ from the coals of other beds in the basin.

A comprehensive study of similar Yunnan Province ores in China (Dai et al., 2018b) based on H and O isotopes led the authors to believe that both colder surface waters and deeper thermal waters were involved in their formation. The leaching of Nb, Zr, and REE took place due to acid rain caused by the release into the atmosphere of HF, HCl, S, and corresponding oxides (CO_2, SO_2) from volcanoes. In our case, such a model is not applicable. The distribution zone for Nb, Zr, and especially REE, over the rock interlayer exceeds 15 cm and even 30–50 cm (Seredin, 1994; Arbuzov et al., 2000). Taking into account coalification this thickness corresponds to 1.5–3-meter thickness of initial peat above the ash horizon. The formation of such a peat thickness took place over a significant time span, possibly for no less than 1000 years. In addition, the role of sulfur in the coals of this seam is very limited. It is indicated not only by its low gross content in the coal, but also by the widespread occurrence of native minerals. Sulfates (barite, etc.) in the coal are also unimportant. Obviously, there is a different mechanism for the redistribution of Nb, Zr, REE, and other elements from the rock interlayer within the coal seam, both above and below the interlayer.

The distribution described above could occur due to sodium bicarbonate groundwaters formed in the basin because there is increased migration of Nb, Zr, and REE especially, as the salinity increases (Lepokurova, 2018a). Such waters are formed in coal basins at an early stage in the formation of coal-bearing sediments. They are also widespread in Kuzbass (Shvartsev et al., 2011). Based on the features of the Nb and Zr distribution in the seam section, it is possible to assume an intensive migration of these elements from the rock interlayer into the host coal. Since the significant enrichment of these elements was noted above the interlayer, as well as under it, we can confidently conclude that the migration took place because of water solutions. The sodium bicarbonate composition of the water is confirmed by REE carbonates present among the newly formed minerals, as well as by the stability of primary albite and secondary albite formation.

Participation of hydrothermal waters in this process in the study area is unlikely. One of the criteria indicating the participation of hydrothermal water is the increased value of $\delta^{18}O$ (Dai et al., 2018b). As determined for Kuzbass, the prolonged interaction of supergene Na-enriched water with the coal and aluminosilicate rocks leads not only to their increased salinity, but also to a significant shift in the isotopic relations in the direction of $\delta^{18}O$ weighting by 2-7‰ and $\delta^{13}C$ by 15-55‰ (Lepokurova, 2018a, 2018b; Shvartsev et al., 2016). This increases when the temperature rises (Lavrushin, 2012).

The time of the formation of the enrichment zone associated with the rock interlayer is limited to the period from the peat bog formation to its transformation into bituminous coal. Studies have shown (Xin et al., 2019) that effective porosity of coal sharply decreases with the maturation to the stage of the increased reflectivity of vitrinite in oil immersion above R_o = 0.5%. In our case, R_o in different sections varies from 1.21% to 1.45% (Table 1). Accordingly, the migration capacity of the elements in water solutions in the coal seam is also sharply reduced. The migration capacity of Ta, Hf, Ga, Sn, Th, and U in this environment is significantly lower due to their chemical properties than that of Nb, Zr, and REE. Therefore, they form only local halos close to the rock interlayer.

Such an active role of the thin rock interlayer in the enrichment of the coal seam by rare metals implies its specific primary composition with a unique enrichment by some of the studied elements. In this connection, the origin of this rock interlayer in seam XI requires special consideration.

4.2. Origin of the rock interlayer in seam XI

It follows from the above discussion that the nature of the rock interlayer formation is the key to understanding the conditions of

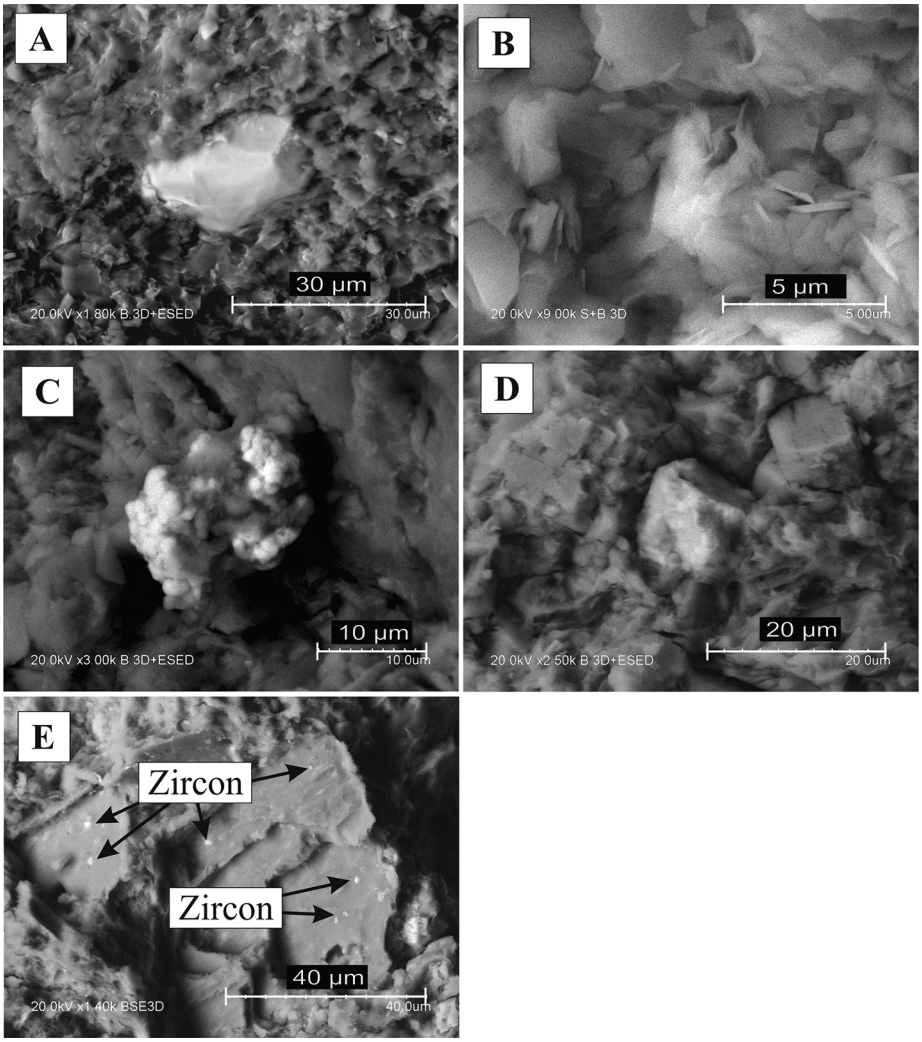

Fig. 11. Zirconium and niobium minerals in the rock interlayer of the seam XI. A – relict crystal of zircon; B – laminar anatase aggregates with Nb and Zr (white); C-spherulitic zirconium oxide (baddeleyite) emissions; D – Ti-Nb-Zr-O crystal; E – microinclusions of zircons in mica scales.

metalliferous coal formation of the seam XI.

Mineralogical and petrographic studies show that the accumulation of mineral matter in the rock interlayer is likely to have occurred by airborne means and not as a result of water transport. There is an absence of structures and textures indicative of transport by water. There is a lack of stratification and grains are angular and randomly orientated. In part, identifying how the rock interlayer formed is complicated by later processes of replacement of primary minerals with kaolinite, hydro-mica, and siderite. No traces of primary volcanic glass were found. The vitroclastic structure in the rock is also not recognized, which may be due to the intensive development of newly formed hydromica and siderite. Mineral aggregates with relic structure of lapilli or, more often, accretionary lapilli (Fig. 8E; Fig. 9 B, C) were identified, although these are now composed of clay minerals. They are currently composed mainly of smectite and can reflect the primary volcanogenic origin. In terms of chemical composition, they are similar to volcanic glass of felsic (rhyolite) composition (Fig. 9).

The geochemical characteristics of the rock interlayer differ significantly from other coal-bearing rocks of the southern Kuzbass. Even in its present state, without taking into account leached elements, the interlayer is anomalously enriched with Ta, Nb, Zr, Hf, Y, REE, Ga, Sn, Th, and other elements. At an early stage of the research this horizon was considered as a specific terrigenous sedimentary rock. The geochemical characteristics of the rock itself and the adjacent coals with abnormal concentrations of Ta, Nb, Zr, Hf, Ga, REE, Th, and U was linked to features of the composition of source rocks in the coal accumulation basin (Seredin, 1994; Arbuzov et al., 2000). In many respects, such an interpretation was logical due to the widespread occurrence of alkaline granitoids, alkaline effusives, and even carbonatite complexes around the Kuzbass region (Fig. 1).

However, as the analysis in this work of the new mineralogical and geochemical data show, this relatively thin horizon (6–15 cm) in the coal seam differs significantly in its characteristics from the underlying and overlying sediments formed from the source rocks. The interlayer is anomalously enriched with Ta, Nb, Zr, Hf, Ga, REE, Th, and U. Concentrations of some elements reach commercially significant values. Thus, the Ta concentration reaches 71 ppm in some parts with an average value of 45 ppm for more than 20 km, whereas the underlying and overlying sediments of seam XI are characterized by normal concentrations of these elements (Table 4).

Such an abnormal accumulation of this range of hydrolysate elements in the sedimentary process is normally only possible in placer-forming processes. However, the formation of placers in the coal formation process is not typical (Yudovich and Ketris, 2002). In addition, the metal-bearing horizon has a significant areal abundance and a relatively low thickness, which are not features of placer deposits. At present the interlayer is traced by detailed transects with geochemical data for more than 20 km in the sublatitudinal direction and more than 5.8 km in the submeridional direction. The total length of the horizon from east to west exceeds 50 km and the area covered is 290 km^2. The

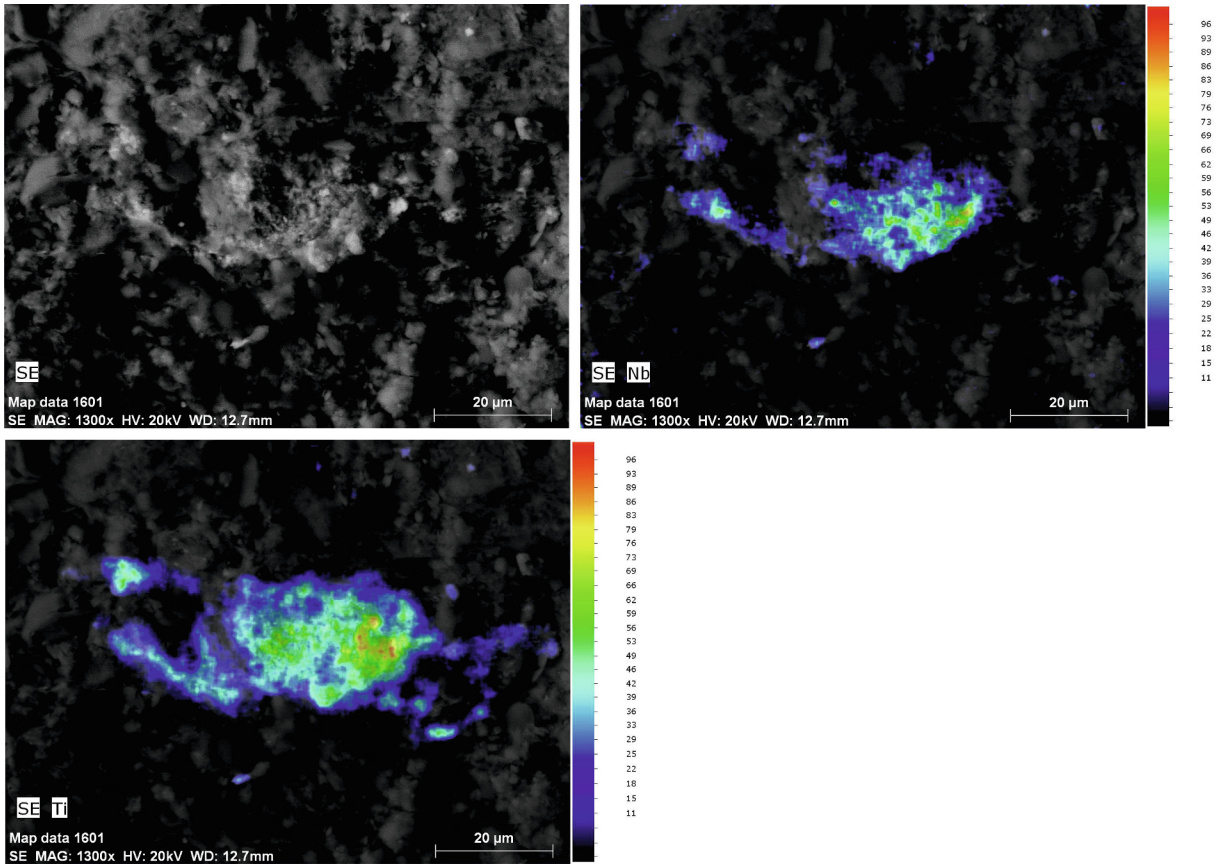

Fig. 12. Titanium oxide earthy aggregate with Nb and Zr admixture. A – picture, B, C – distribution of Nb and Ti.

formation of such a contrasting thin horizon over such a large area, with the absence of a clearly pronounced stratification, is only possible as a result of a catastrophic phenomenon. The only possible mechanism for such a simultaneous arrival of material so different in composition to the normal detrital sediment associated with the coals has to be a rather catastrophic volcanic eruption. The absence of stratification is consistent with an ash fall over a short period of time.

Another important feature is the significant enrichment of the coal with Ta, Nb, Zr, Hf, Ga, REE, Th, and U at the contact with the rock interlayer. This indicates the redistribution of elements during coal formation. It is not possible to determine the time of the redistribution: peat accumulation, diagenesis, and catagenesis, but the coal enrichment features suggest that the primary source was the rock interlayer. The recalculation of the element concentrations in the rock interlayer, taking into account the alkaline matter, shows that the initial composition of the interlayer rocks corresponded to the comendites-pantellerites (Table 5). These rocks are felsic, sometimes ultra-felsic, but highly alkaline.

Dai et al. (2017) identified four groups of altered volcanic ashes (tonsteins) in coals: felsic, medium, mafic, and alkaline. Applying their criteria the volcanogenic interlayer in the seam XI corresponds to an ash of felsic composition, but highly alkaline. On the one hand, in terms of silica content, these are rocks of the rhyolite group. The presence of free silica in the form of quartz, cristobalite and trydimite also confirms the felsic composition of the initial ash (Table 3). The presence of secondary accumulations of globular and lamellar quartz in the coals at the contact with the interlayer (Fig. 10) indicates a partial loss of silica from the initial pyroclastics during its transformation possibly in a sodium bicarbonate groundwater. This indicates that the initial silica content was even higher. The coal ash at the contact with the

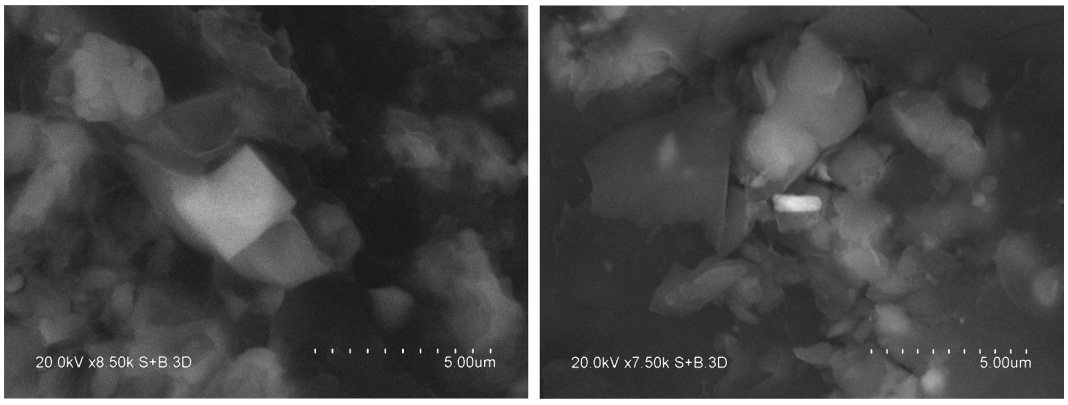

Fig. 13. Zircon crystals (white) in aluminosilicate matter of coal.

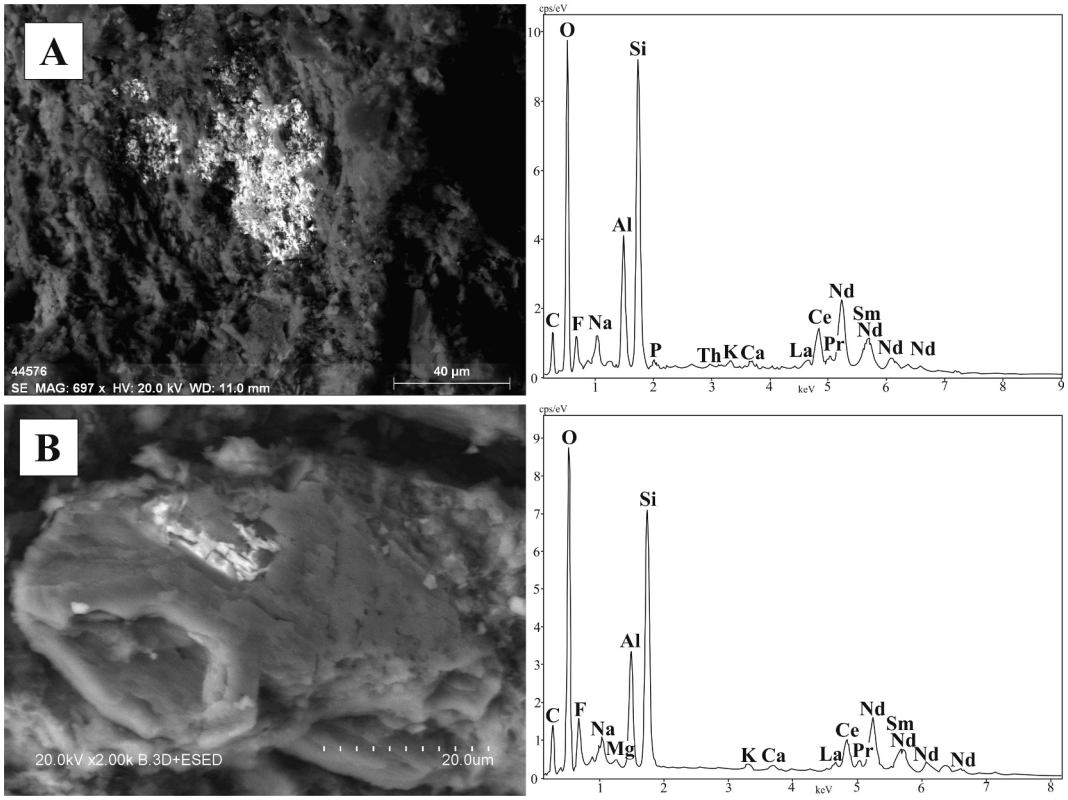

Fig. 14. Neodymium bastnesite: A – in the fine-grained basic mass; B – in the pores in the albite crystal.

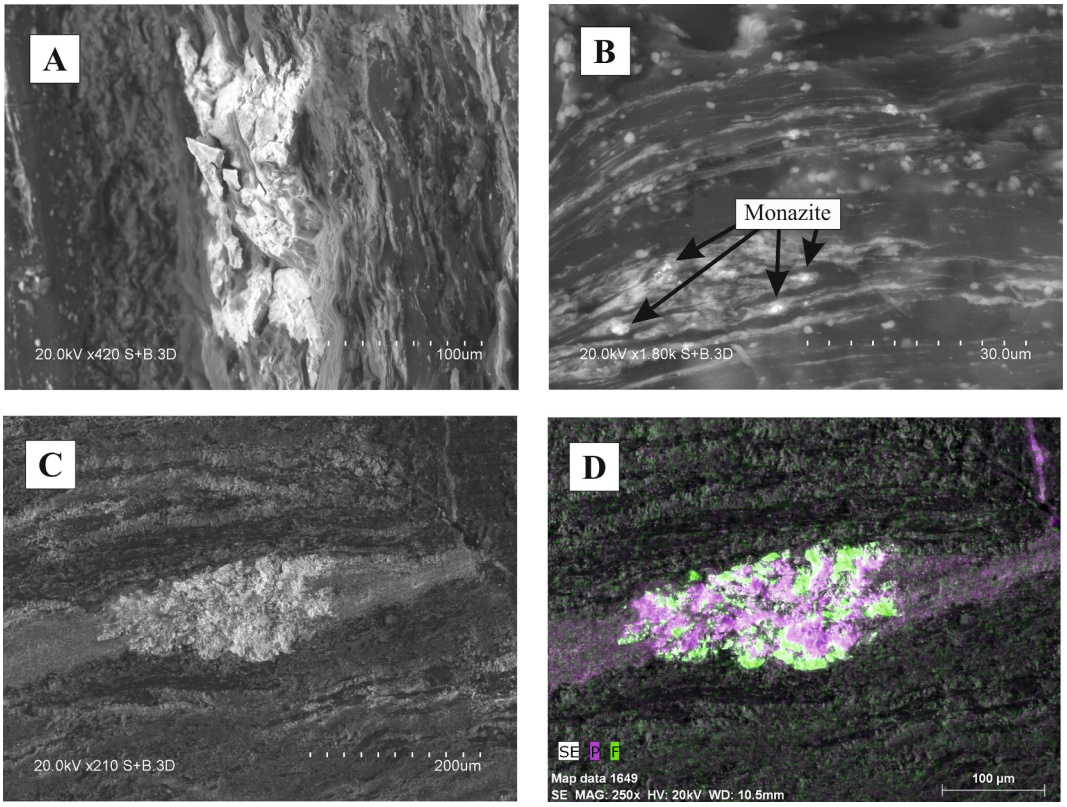

Fig. 15. Rare earth minerals in the coal at the contact with the tonstein: A – bastnasite; B – nodular monazite; C – monazite and REE fluorocarbonate aggregate in the coal and D – distribution of phosphorus and fluorine.

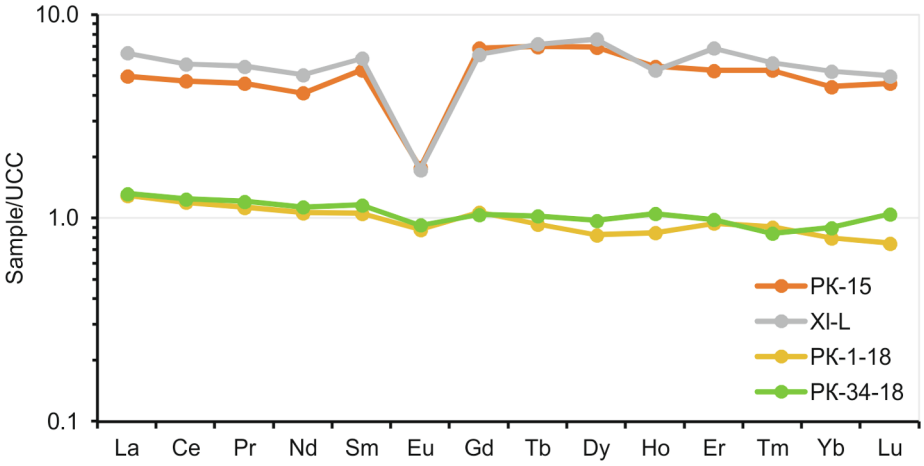

Fig. 16. Normalized graphs of REE distribution in the interlayer of the seam XI (Kuzbass) and in the roof and bottom coal-bearing rocks. REE concentrations are normalized to the mean concentration in the upper continental crust (after Taylor and McLennan, 1985). 1 – sample PK-15, interlayer of the seam XI, Raspadsky cut; 2 – sample XI-L, interlayer of the seam XI, Lenin mine; 3 –sample PK-1–18, roof of the seam XI; 4 – sample PK-34–18, bottom of the seam XI.

volcanogenic interlayer contains from 78 to 81% of SiO_2. On the other hand, abnormally high concentrations of Ta, Nb, Zr, Hf, Ga, and REE indicate the alkaline composition of the initial rocks (Solodov et al., 1987). In this connection, the pyroclastic horizon in the seam XI is compositionally similar to volcanic rocks and tonsteins of both alkaline and felsic composition. However, in this case, the term tonstein or meta-tonstein is not applicable because the small fraction of kaolinite and mixed-layer clay minerals amounts to less than 30% in total (Table 3).

TiO_2/Al_2O_3 varies within narrow limits and is about 0.026–0.027 for the studied samples. According to Spears (2012), such a value is typical of intermediate volcanogenic rocks, but in this case it is quite close to felsic rocks (< 0.020). It is important to mention that this ratio plays an auxiliary role in determining the composition of volcanic rocks. For example, felsic alkaline volcanics such as pantellerites are characterized by rather high values (0.04–0.06) of this ratio (White et al., 2009).

The diagrams of REE distribution, normalized to the mean in the upper continental crust, in the studied rock interlayer differ significantly from the normalized curves in the roof rocks and bedrocks (Fig. 16). The bedrock and overlying rocks have similar normalized curves and, accordingly, have a common source for the mineral matter, which is similar to the composition of medium grain-size clastic sedimentary rocks. The interlayer is characterized by a completely different type of the graph (Fig. 16). This indicates a different source for its formation and, together with the data considered earlier, confirms the volcanogenic nature of this rock interlayer in the coal seam. The features of REE distribution graphs normalized to chondrite in the postulated volcanogenic interlayer of the seam XI testifies to the felsic composition of the initial volcanogenic pyroclastics. This is supported by the presence of a clearly pronounced Eu minimum (Fig. 17). The value of the Eu anomaly for different samples is Eu/Eu* = 0.18–0.19. A similar value was obtained for the Fire Clay tonstein, whose initial composition of the volcanogenic pyroclastics was determined as rhyolite (Lyons et al., 1992).

In general, the interlayer in the seam XI has a very similar REE to the tonstein from the well documented Fire Clay seam (Fig. 17). The interlayer differs with slightly higher REE concentrations and, especially, by higher concentration of heavy REE. The La-Yb ratio in the interlayer of the seam XI is 14–16, while in the Fire Clay tonstein it is 36.5, although there are areas where the ratio is lower (Hower et al., 1999) and closer in composition to the interlayer in this work.

The normalized plots are even closer to the alkaline tonsteins of Permian age in the north of Hubei province (Zhou et al., 2000). They are close to each other both by the form of normalized graphs and by the value of Eu anomaly.

From the features of the normalized curve, the interlayer of the seam XI is closest to pantellerites from the area of their prototype in Pantelleria, Italy (White et al., 2009) and pantellerites from the Ulan-Tologoy complex, Mongolia (Yarmolyuk et al., 2016). In the first case, a slightly less contrasting negative Eu anomaly (Eu/Eu* = 0.38–0.52) is characteristic; whereas, in the second case, the anomaly is more contrasting (Eu/Eu* = 0.04–0.05). This feature of the normalized curve of the seam XI interlayer is also close to that of the pantellerite tuffs (Eu/Eu* = 0.10) of central Mongolia (Andreeva and Kovalenko, 2011). Mongolian pantellerites and pantellerite tuffs have TiO_2/Al_2O_3 of 0.029 and 0.024, respectively, which is the same as for the studied rock interlayer in the seam XI. In terms of mineral and chemical composition, the pantellerites of central Mongolia and western Tuva could be considered as a source of matter for the formation of the interlayer in the seam XI, but, according to the isotopic studies, they are related to the Carboniferous and Lopingian volcanic rocks (Andreeva and Kovalenko, 2011; Yarmolyuk et al., 2016). According to published data, the isotopic age of the pantellerites and granites in northwestern Mongolia, determined by $^{40}Ar/^{39}Ar$ and Sm-Nd methods for the Ulan-Tologoy complex, is close to 298 million years, which is somewhat older than the estimated geological age of the seam XI.

Another geochemical feature of the rock interlayer in the seam XI is the abnormally high concentrations of Nb, Ta, Zr, Hf, and, to a lesser extent, Ga, Th, and U. This range of elements is typical for alkaline rocks. As described in alkaline volcanogenic tonsteins in China (Zhou et al., 2000; Dai et al., 2014, 2017) and in ash horizons outside coal deposits (Dai et al., 2010). Absolute values of the concentrations of these elements in the relatively thin rock interlayer in the coal, in general, do not fully correspond to their concentrations in the original rock due to a significant redistribution of the elements in the process of the coal seam formation. A number of elements are actively leached out of the interlayer and are lost from the system. Consequently the concentrations of relatively inactive hydrolysate elements, such as Al, Nb, Ta, Zr, Hf, Sc, and others, are increased.

According to Lyons et al. (1992), the concentration of these elements in the process of kaolinitization of volcanic pyroclastics increases by a factor of about 2.7 for the Fire Clay tonstein. The exact value is difficult to obtain because migration of the hydrolysate elements does take place leading to some potential loss from the original ash. To some extent element ratios can be used to determine the composition of the original rock. A good example is the diagram of Zr/TiO_2 and Nb/Y (Winchester and Floyd, 1977). The use of this diagram is possible if it is assumed that the migration of these elements is limited and, more importantly, uniform for each pair of the elements. Studies in recent decades have shown that the migratory capacity of these two pairs of elements may differ in some cases, which may lead to misinterpretation of the data obtained (Arbuzov et al., 2017). On the other hand it has also been noted that, although igneous designations may not be exact,

Table 4
Rock-forming oxides (%) and minor elements (ppm) in the coal-bearing rocks and in the interlayer of the seam XI.

Element	Roof	Floor (Soil)	Average siltstone[1]	interlayer	CC[2]
SiO_2	70.0	64.2	67.1	57.2	0.9
TiO_2	0.57	0.72	0.64	0.50	0.8
Al_2O_3	13.8	17.1	15.5	19.0	1.3
Fe_2O_3	1.59	1.61	1.60	2.97	2.0
MnO	0.017	0.014	0.016	0.028	1.9
CaO	0.26	0.31	0.28	0.36	1.3
Mg0	0.87	0.88	0.88	1.15	1.4
K_2O	2.5	2.8	2.6	1.4	0.6
Na_2O	1.5	1.4	1.5	1.9	1.3
P_2O_5	0.09	0.13	0.11	0.10	1.0
LOI	8.8	10.8	9.8	15.4	
Li	20.1	19.7	19.9	49.7	2.5
Be	3.0	4.4	3.7	14.5	3.9
Sc	12.8	12.0	12.4	7.9	0.6
V	88.9	90.0	88.0	49.6	0.6
Cr	114	104	109	79.6	0.7
Co	9.4	5.4	7.4	14.7	2.0
Ni	31.5	20.7	26.1	25.6	1.0
Cu	51.9	101	76.3	60.5	0.8
Zn	89.2	106	97.4	291	3.0
Ga	21.8	22.8	22.3	80.6	3.6
Ge	1.8	1.8	1.8	3.9	2.2
As	4.5	1.7	3.1	6.9	1.1
Se	1.5	1.2	1.3	7.8	5.8
Rb	114	121	117	81.6	0.7
Sr	153	203	178	205	1.2
Y	24.2	26.9	25.5	118	4.6
Zr	225	261	243	1910	7.9
Nb	13.6	14.9	14.2	264	18.5
Mo	2.4	2.1	2.3	0.8	0.3
Ag	0.7	0.3	0.5	3.2	6.5
Cd	0.3	0.5	0.4	2.6	6.9
Sn	2.9	2.7	2.8	36.7	12.8
Sb	0.7	0.6	0.7	1.5	2.4
Cs	7.3	8.4	7.9	5.8	0.7
Ba	519	598	558	565	1.0
La	40.1	40.9	40.5	149	3.7
Ce	80.0	83.1	81.5	302	3.7
Pr	8.9	9.5	9.2	32.6	3.5
Nd	32.3	34.4	33.3	107	3.2
Sm	6.3	6.9	6.6	24.0	3.6
Eu	1.1	1.2	1.1	1.6	1.4
Gd	5.9	5.7	5.8	26.0	4.5
Tb	0.8	0.9	0.8	4.4	5.4
Dy	4.6	5.4	5.0	24.2	4.9
Ho	0.9	1.1	1.0	4.4	4.5
Er	3.1	3.2	3.2	12.2	3.9
Tm	0.5	0.4	0.4	1.8	4.0
Yb	2.5	2.8	2.6	9.7	3.7
Lu	0.3	0.5	0.4	1.5	3.6
Hf	6.9	6.7	6.8	76.3	11.2
Ta	1.1	0.6	0.8	56.4	67.1
W	2.7	4.1	3.4	2.7	0.8
Hg, ppb	28.6	35.9	32.2	763	23.7
Tl	0.6	0.8	0.7	0.9	1.2
Pb	22.0	26.3	24.1	39.7	1.7
Th	12.5	12.9	12.7	80.7	6.4
U	4.0	3.4	3.7	15.8	4.3
ΣREE	187	196	192	700	3.7
Th/U	3.1	3.8	3.7	5.1	

Note: 1 – Average of roof and floor clastic sediments; 2 – ratio of the element concentrations in the interlayer to the concentration in the host rock.

broad classifications are possible (Spears and Arbuzov, 2019).

In the presentation of data for specific rocks in the Zr/TiO_2 and Nb/Y diagram, it was noted that tonsteins are often in the field of more basic and less alkaline composition than the initial volcanic ashes. The reason for this is more active leaching of Nb and Zr from the tonsteins compared to Y and Ti during the transformation of volcanic ash. Different mobility of these elements during the transformation of basic volcanics into tonsteins was convincingly demonstrated by Spears and Arbuzov (2019), when comparing the Jersey Yellowstone tonstein with the initial volcanic rocks. According to these data, the fully developed kaolinite tonstein is enriched with hydrolysate elements, such as Al, Ti, Zr, Y, Sr, and Nb due to the leaching of mobile elements from the primary ash. The accumulation coefficients in the tonstein compared to the initial rock are as follows: Al – 2.26, Ti – 2.18, Y – 2.16, Sr – 2.15, Zr – 0.87, and Nb – 1.67. On the basis of these data there is no doubt that the mobility of Zr and Nb in this process was significantly higher than that of Y and Ti.

Table 5
Concentrations of Zr, Hf, Nb, Ta, REE, Ga, Th, and U in the rock interlayer of the seam XI, the Fire Clay tonstein and in some types of rare-metal volcanogenic rocks, ppm.

Sampling site	Zr	Hf	Nb	Ta	ΣREE + Y	Ga	Th	U
Seam XI (PK-15–18)	1915	66.4	264	50.5	818	80.6	70.2	13.8
Seam XI (XI-Л)	1919	72.8	197	31.3	1009	61.5	67.1	14.8
Seam XI, Shevyakov mine[1]	901.7	59.7	210	46.3	865.1	nd	69.3	24.6
Seam XI, Lenin mine	1607	43.5	151	41.9	873.0	42.0	61.0	28.0
Tonstein Fire Clay	441	18.5	18.2	1.8	874.3	28.7	60.3	15.7
Tonstein Fire Clay[2]	700	20.0	30.0	3.0	564.3	48.0	66.0	17.0
Huayingshan, Sichuan, China[3]	1577	76.3	235	29.3	1403.0	78.5	95.0	17.6
Pantellerite, Italy[4]	1641	37.3	281	22.5	1046.5	35.0	33.0	9.9
Pantellerite, Italy[4]	1926	46.2	339	24.7	1382.7	33.0	35.3	11.4
Pantellerite, Mongolia [5]	3533	59.5	169	9.8	1354.4	nd	74.0	15.8
Pantellerite, Mongolia [5]	2234	59.0	124	8.9	993.5	nd	44.7	5.5
Sedimentary rock[6]	170	3.9	7.6	1.0	164.4	12	7.7	3.4

Note: nd – no data available, 1 – Seredin, 2004; 2– Hower et al, 1999; 3– Dai et al., 2014; 4– White et al., 2009; 5– Andreeva and Kovalenko, 2011; 6 – Grigorev, 2003.

In the Winchester-Floyd diagram, the studied interlayer in the seam XI, selected in two spatially distant sections, is located in the field of comendite-pantellerite (volcanogenic rocks of felsic composition of the alkaline variety) and some samples are in the field of trachytes (alkaline rocks of medium composition) (Fig. 18).

Analysis of Table 5 shows that the pantellerite tuff of central Mongolia can be considered as a possible source of primary volcanogenic material for the rock interlayer in the seam XI. Such a conclusion can be made taking into account the different mobility of elements during the ash transformation. Of the relatively inert petrogenic elements, fourfold concentrations of Ti and Al were noted. The same accumulation coefficient was also noted for Ta. The accumulation coefficients of U, Th, Hf, and Nb are higher than 1. For Zr and Y the coefficients are close to 1. Taking into account the specifics of the interlayer material transformation in the seam XI, these results are in good agreement with the data on the mobility of these elements in the transformation of volcanogenic pyroclastics, obtained by Spears and Arbuzov (2019). The extent of the mineral substance transformation for the volcanic-sedimentary rocks in the seam XI is significantly lower than that for the tonsteins, so the concentration coefficients are lower, but the general regularities of different mobility of these most inert components in this process is present. These data are in good agreement with the results of other research methods.

Thus, the geochemical data obtained allows us to confidently conclude that the rock interlayer in the seam XI, which is a source for the accumulation of rare elements in the coals, is represented by geochemically modified ash of pantellerite composition. The absence of primary transformation of the volcanogenic material in the hypergenesis zone before it enters the peat deposit ensured the preservation of its rare-metal potential and further redistribution in the coal seam forming the commercial Nb-Ta-Zr-Hf-Y-REE-Ga mineralization.

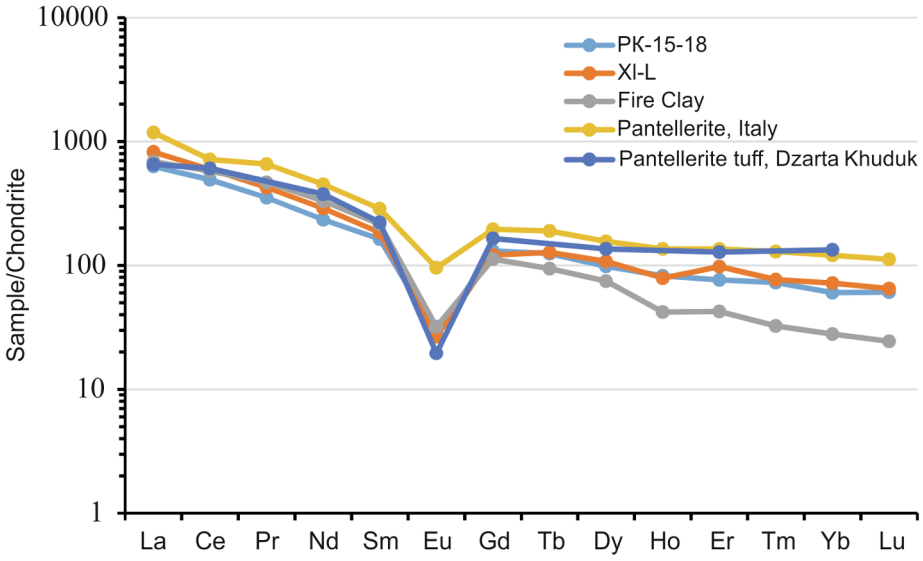

Fig. 17. Normalized graphs of REE distribution in the tonstein of the seam XI (Kuzbass), in the Fire Clay tonstein (Kentucky, USA), in the pantellerite from Pantelleria, Italy (White et al., 2009), and in the pantellerite from the Ulan-Tologoy complex, Mongolia (Yarmolyuk et al., 2016). Normalized to chondrite (McDonough and Sun, 1995). 1 – tonstein of the seam XI, sample PK-15, Raspadsky cut; 2 – tonstein of the seam XI, sample XI-L, Lenin mine; 3 – Fire Clay tonstein; 4 – pantellerite from the Ulan-Tologoy complex, Mongolia; 5 – pantellerite from Pantelleria region, Italy.

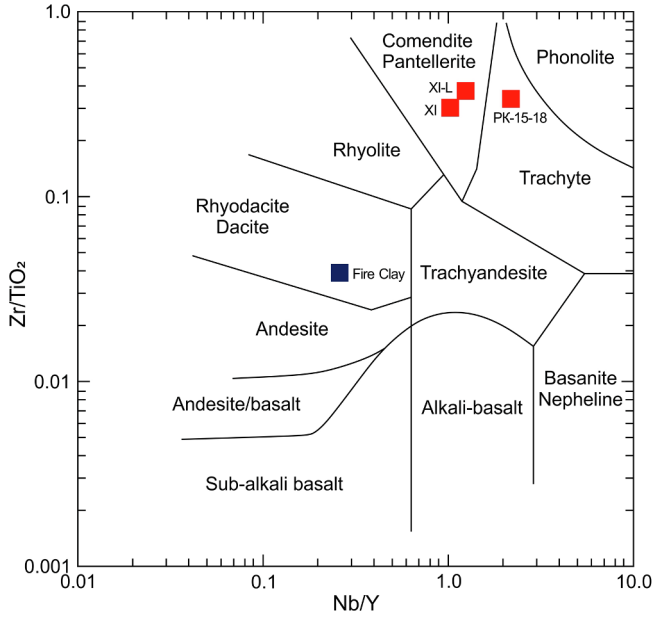

Fig. 18. Location of the pyroclastic interlayer in the seam XI according to the Winchester and Floyd (1977) classification diagram by Zr/TiO_2 and Nb/Y. XI-L, PK-15 – separate samples from the Lenin mine and Raspadsky cut, XI – average composition of the pyroclastic interlayer (8 samples); FC-1 – tonstein sample from the Fire Clay seam.

4.3. Metal resources in the coal

The analysis has shown that the coal of seam XI has uniquely high Nb and Ta concentrations for coals. The mean Nb concentration in the seam is more than twice as high as even the highest minimum suggested (cut-off grade) commercial values for rare-metal-coal deposits (Seredin, 2004; Dai and Finkelman, 2018). In local sites, where the thickness near the interlayer is 15–20 cm, their concentrations in the coal are generally several times higher than the commercial minimum, about 0.2% on average.

Tantalum is mainly concentrated in the volcanogenic interlayer, or directly in contact with it. The mean concentration in the coal ash of seam XI, including the rock interlayer is 26.9 ppm of Ta_2O_5, whereas its concentration in the interlayer exceeds 68 ppm, and in some sections it reaches 87 ppm.

Zirconium concentrations in the same ores (in the coal ash) also correspond to their minimum commercial values, although it is not as significant as Nb concentration (Table 6).

Table 6
Concentrations of the resources of rare metals oxides in the seam XI.

Oxides	Concentration in the ash, ppm		Resources, tonnes	
	I	II	I	II
Nb_2O_5	930	689	26,145	31,545
ZrO_2	2526	2365	71,024	108,281
$\Sigma REE + Y_2O_3$	975	934	27,423	42,763
Ta_2O_5	8.4	26.9	237	1232
HfO_2	37.5	49.6	1054	2271
Ga_2O_3	48.5	69.4	1365	3178

Note: I – coal without the rock interlayer; II – the entire seam with the rock interlayer

In addition to Nb, Ta, Zr, and Hf, the ores are enriched in REE. The sum of REE and Y in terms of oxides is 975 ppm. Such REE concentrations are not significant in case of light REE prevalence, but may be significant in the processing of complex ores. Similarly, we consider Ga, the concentration of which ranges from 48.5 to 69.4 ppm, depending on whether or not the interlayer is taken into account in the calculation. In the latter case, the concentration is 1.5-times higher. Therefore, when calculating the mean concentrations and resources of valuable metals in the volcanogenic interlayer, the mean Ta, Hf, and Ga concentrations and resources of all considered metals increase (Table 6).

Metal resources calculated for eight studied sections are presented in Table 6. In the calculation the average seam thickness was assumed to be 1.5 m, the thickness of the volcanogenic interlayer – 0.1 m, the distance along the strike – 21 km, the distance down dip – 5.8 km, the density of the coal mass – 1.35 g/cm^3, the density of the rock interlayer – 2.2 g/cm^3, the average ash yield of the coal – 11.4%, including the interlayer – 17.9%.

It follows from these data that the coals of seam XI form an average scale deposit of complex ores with significant concentrations of valuable elements. Profitability of their processing can be achieved by selective extraction of coal from this seam, using high-energy coal as fuel in a small thermal power plant. There are no restrictions of the use of this coal in the energy sector. The resulting ashes and slags, when subject to complex processing could lead to the extraction of a group of valuable elements.

5. Conclusions

The coals of seam XI are polymetallic ores of Nb-Ta-Zr-Hf-Y-REE-Ga composition. Their formation is associated with the presence of thin (6–15 cm) non-coal interlayer in the coal seam. This interlayer is enriched with Nb, Ta, Zr, Hf, Y, REE, Ga, Th, U, Sn, and other lithophilic elements. The geochemical features of this interlayer and the composition of relict minerals make it possible to link this horizon to the arrival of felsic volcanogenic pyroclastic matter of alkaline composition during the peat accumulation. The restored composition of the composition of the volcanogenic pyroclastics of these rock interlayers corresponds to the family of comendite-pantellerites.

A possible source is pantellerite ash from Mongolia or southeast Siberia. They are enriched in Nb, Ta, Zr, Hf, Y, REE, Ga, Th, and U. In the process of coalification, rare elements-hydrolysates were redistributed and rare-metal mineralization in coal resulted. The redistribution occurred at the early stages of coalification with the involvement of sodium bicarbonate groundwaters. The distribution of these elements in the coal and coal ash in the vertical section of the coal seam emphasizes their connection with the volcanogenic pyroclastic horizon and reflects the geochemical zoning caused by the redistribution of chemical elements in the groundwater. This is especially evident for REE and is clearly visible in the analysis of the normalized graphs relative to chondrite and upper continental crust. Individual elements (Ta, Hf, and Ga) from the ore spectrum differ in their weak migration capacity and accumulate in the volcanogenic interlayer or in close to it.

The ore substance is mainly concentrated in the fine mineral phase, essentially Zr-Nb-Ti-Fe oxides, fine zircons, and rare-earth carbonates (bastnasite) and phosphates (monazite, xenotime, goyazite). Some of the elements are contained in a scattered form in the organic matter. The epigenetic nature of the majority of minerals is clearly visible in their distribution in the coal matrix, relation to the pore space, presence of micro-veinlets, and to the areas of the volcanogenic interlayers.

Metals resources (Nb, Ta, Zr, Hf, Y, REE, and Ga) in the seam XI make it a medium-resource deposit.

The research that has been undertaken enables exploration criteria to be developed to identify this type of mineralization. A characteristic feature of such ores is the presence of a horizon of volcanogenic pyroclastic rocks of alkaline composition with increased radioactivity. The presence of such a horizon was noted in similar ores in China (Dai et al., 2010, 2012b, 2014) and in the coals of the Minusinsky Basin (Arbuzov et al., 2003). This feature allows such horizons to be identified by gamma-ray logging at an early stage in coalfield exploration.

The connection of complex Nb-Ta-Zr-Hf-Y-REE-Ga mineralization with alkaline volcanogenic pyroclastics significantly expands the prospects of further similar discoveries in coals of East and Central Asia. High volcanic activity of this period coupled with the alkaline magmatism (Yarmolyuk et al., 2013) contributed to the formation of metal-bearing ash horizons and when buried in paleo-bogs, complex rare-metal-coal deposits were formed. The disparate locations of known ores in the vast territory of China and Russia suggest that a number of other such deposits may be discovered by systematic studying sedimentary basins of this age.

Acknowledgements

The research was carried out under the support of the grant of Russian Science Foundation (Project no. 18-17-00004).

References

Andreeva, I.A., Kovalenko, V.I., 2011. Evolution of magmas of trachydacites and pantellerites of bimodal association of volcanites of the Dzart Khuduk occurrence, Central Mongolia: according to the data of the study of inclusions in minerals. Petrology 19 (4), 363–385 (in Russian).

Arbuzov, S.I., Ershov, V.V., Potseluyev, L.L., Rikhvanov, L.P., 2000. Rare elements in coals of the Kuznetsk Basin. Kemerovo. (in Russian).

Arbuzov, S.I., Ershov, V.V., Rikhvanov, L.P., Usova, T.Y., Kargin, V.V., Bulatov, A.A., Dubovik, N.E., 2003. Rare-Metal Potential of The Coals of the Minusinsk Basin. Siberian Branch of the Russian Academy of Sciences, Geo Branch, Novosibirsk (in Russian).

Arbuzov, S.I., Ershov, V.V., 2007. Geochemistry of Rare Elements in Coals of Siberia. D-Print Publishing House, Tomsk (in Russian).

Arbuzov, S.I., Mashenkin, V.S., Rybalko, V.I., Sudyko, A.F., 2014. Rare-metal potential of coals of Northern Asia (Siberia, Russian Far East, Mongolia). Geol. Mineral Resour. Siberia 3 (2), 41–44 (in Russian).

Arbuzov, S.I., Mezhibor, A.M., Spears, D.A., Ilenok, S.S., Shaldybin, M.V., Belaya, E.V., 2016. Nature of tonsteins in the azeisk deposit of the irkutsk coal basin (Siberia, Russia). Int. J. Coal Geol. 152, 99–111. https://doi.org/10.1016/j.coal.2015.12.001.

Arbuzov, S.I., Ilenok, S.S., Vergunov, A.V., Shaldybin, M.V., Sobolenko, V.M., Nekrasov, P.E., 2017. Mineralogical-geochemical identification of explosive volcanism products in coals of the Minussinsk basin. Petrology of magmatic and metamorphic complexes. Issue 9. Proceedings of 9th All-Russian petrographic conference, CSTI, Tomsk 37. (In Russian).

Babin, G.A., Yuriev, A.A., Bychkov, A.I., Dubsky, V.S., Shchigrev, A.F., 2007. State geological map of the Russian Federation. Scale 1: 1,000,000. Geological map. N 45 (Novokuznetsk). (in Russian).

Belopolsky, M.P., Bunakova, N.Yu., Mikhailova, N.A., Popov, N.P., Skrizhinskaya, V.I., Stolyarova, I.A., Filatova, M.P., Filatova, K.K., Shuvalova, N.I., 1974. Chemical Analysis of Rocks and Minerals. Nedra, Moscow (in Russian).

Bish, D.L., Post, J.E., 1993. Quantitative mineralogical analysis using the Rietveld full-pattern fitting method. Am. Mineral. 78, 932–940.

Bouška, V., Pešek, J., 1999. Quality parameters of lignite of the North Bogemian Basin in the Czech Republic in comparison with the world average lignite. Int. J. Coal Geol. 40, 211–235. https://doi.org/10.1016/S0166-5162(98)00070-6.

Crowley, S.S., Stanton, R.W., Ryer, T.A., 1989. The effects of volcanic ash on the maceral and chemical composition of the C coal bed, Emery Coal Field, Utah. Org Geochem. 14, 315–331.

Dai, S., Zhou, Y., Zhang, M., Wan, G.X., Wang, J., Song, X., Jiang, Y., Luo, Y., Song, Z., Yang, Z., Ren, D., 2010. A new type of Nb (Ta)-Zr(Hf)-REE-Ga polymetallic deposit in the late Permian coal-bearing strata, eastern Yunnan, southwestern China: Possible economic significance and genetic implications. Int. J. Coal Geol. 83, 55–63. https://doi.org/10.1016/j.coal.2010.04.002.

Dai, S., Wang, X., Seredin, V.V., Hower, J.C., Ward, C.R., O'Keefe, J.M.K., Huang, W., Li, T., Li, X., Liu, H., Xue, W., Zhao, L., 2012a. Petrology, mineralogy, and geochemistry of the Ge-rich coal from the Wulantuga Ge ore deposit, Inner Mongolia, China: New data and genetic implications. Int. J. Coal Geol. 90–91, 72–99. https://doi.org/10.1016/j.coal.2011.10.012.

Dai, S., Ren, D., Chou, C.-L., Finkelman, R.B., Seredin, V.V., Zhou, Y., 2012b. Geochemistry of trace elements in Chinese coals: a review of abundances, genetic types, impacts on human health, and industrial utilization. Int. J. Coal Geol. 94, 3–21. https://doi.org/10.1016/j.coal.2011.02.003.

Dai, S., Luo, Y., Seredin, V.V., Ward, C., Hower, J.C., Zhao, L., Liu, S., Zhao, C., Tian, H., Zou, J., 2014. Revisiting the late Permian coal from the Huayingshan, Sichuan, southwestern China: Enrichment and occurrence modes of minerals and trace elements. Int. J. Coal Geol. 122, 110–128. https://doi.org/10.1016/j.coal.2013.12.016.

Dai, S., Liu, J., Ward, C.R., Hower, J.C., Xie, P., Jiang, Y., Hood, M.M., O'Keefe, J.M.K., Song, H., 2015. Petrological, geochemical, and mineralogical compositions of the low-Ge coals from the Shengli Coalfield, China: A comparative study with Ge-rich coals and a formation model for coal-hosted Ge ore deposit. Ore Geol. Rev. 71, 318–349. https://doi.org/10.1016/j.oregeorev.2015.06.013.

Dai, S., Chekryzhov, I., Seredin, V., Nechaev, V., Graham, I., Hower, J.C., Ward, C., Ren, D., Wang, X., 2016. Metalliferous coal deposits in East Asia (Primorye of Russia and South China): a review of geodynamic controls and styles of mineralization. Gondwana Res. 29 (1), 60–82. https://doi.org/10.1016/j.gr.2015.07.001.

Dai, S., Ward, C.R., Graham, C.R., French, D., Hower, J.C., Zhao, L., Wang, X., 2017. Altered volcanic ashes in coal and coal-bearing sequences: A review of their nature and significance. Earth Sci. Rev. 175, 44–74. https://doi.org/10.1016/j.earscirev.2017.10.005.

Dai, S., Finkelman, R.B., 2018. Coal as a promising source of critical elements: Progress and future Prospects. Int. J. Coal Geol. 186, 155–164. https://doi.org/10.1016/j.coal.2017.06.005.

Dai, S., Yan, X., Ward, C.R., Hower, J.C., Zhao, L., Wang, X., Zhao, L., Ren, D., Finkelman, R.B., 2018a. Valuable elements in Chinese coals: a review. Int. Geol. Rev. 60 (5–6), 590–620. https://doi.org/10.1080/00206814.2016.1197802.

Dai, S., Nechaev, V.P., Chekryzhov, I.Yu., Zhao, L., Vysotskiy, S.V., Graham, I., Ward, C.R., Ignatiev, A.V., Velivetskaya, T.A., Zhao, L., French, D., Hower, J.C., 2018b. A model for Nb-Zr-REE-Ga enrichment in Lopingian altered alkaline volcanic ashes: Key evidence of H-O isotopes. Lithos 302–303, 359–369. https://doi.org/10.1016/j.lithos.2018.01.005.

Grigorev, N.A., 2003. Average concentrations of chemical elements in rocks of the upper continental crust. Geochem. Int. 41 (7), 711–718.

Hower, J.C., Ruppert, L.F., Eble, C.F., 1999. Lanthanide, yttrium, and zirconium anomalies in the Fire Clay coal bed, Eastern Kentucky. Int. J. Coal Geol. 39 (1–3), 141–153. https://doi.org/10.1016/S0166-5162(98)00043-3.

Hower, J.C., Eble, C.F., Dai, S., Belkin, H.E., 2016. Distribution of rare earth elements in eastern Kentucky coals: Indicators of multiple modes of enrichment? Int. J. Coal Geol. 160–161, 73–81. https://doi.org/10.1016/j.coal.2016.04.009.

Hu, R.Z., Qi, H.W., Zhou, M.F., Su, W.C., Bi, X.W., Peng, J.T., Zhong, H., 2009. Geological and geochemical constraints on the origin of the giant Lincang coal seam-hosted germanium deposit, Yunnan, SW China: A review. Ore Geol. Rev. 36, 221–234. https://doi.org/10.1016/j.oregeorev.2009.02.007.

Ketris, M.P., Yudovich, Ya.E., 2009. Estimations of Clarkes for carbonaceous biolithes:

world average for trace element contents in black shales and coals. Int. J. Coal Geol. 78, 135–148. https://doi.org/10.1007/s11631-015-0053-7.
Lavrushin, V.Yu, 2012. Subsurface fluids of the Greater Caucasus and its surrounding. GEOS, Moscow (in Russian).
Lepokurova, O.E., 2018a. Soda underground waters of southeastern West Siberia: geochemistry and formation conditions. Dissertation of doctor of geol-miner. Sciences. Tomsk (in Russian).
Lepokurova, O.E., 2018. Sodic groundwaters in the southern Kuznetsk Basin: isotopic and chemical characteristics and genesis. Geochem. Int. 56 (9), 934–949. https://doi.org/10.1134/S0016702918090069.
Lin, M., Bai, G., Duan, P., Xü, J., Duan, D., Li, Z., 2013. Perspective of comprehensive exploitation of the valuable elements of Chinese coal. Energy Explor. Exploit. 31 (4), 623–627. https://doi.org/10.1260/0144-5987.31.4.623.
Lyons, P.C., Outerbridge, W.E., Triplehorn, D.M., Evans, H.T., Congdon, R.D., Capiro, M., Hess, J.S., Nash, W.P., 1992. An Application isochron: A caolinized Carboniferous air-fall volcanic-ash deposit (tonstein). Geol. Soc. Amer. Bull. 104, 1515–1527.
McDonough, W.F., Sun, S., 1995. The composition of the Earth. Chem. Geol. 120, 223–253.
Moore, D.M., Reynolds Jr., R.C., 1997. X-ray Diffraction and the Identification and Analysis of Clay Minerals. Oxford University Press, Oxford.
Nifantov, B.F., Artemyev, V.B., Yasyuchenya, S.V., Anferov, B.A., Kuznetsov, L.V., 2014. Geochemical and Geotechnological Substantiation of New Directions in the Development of Kuzbass Coal Deposits. Mining Publishing House “Commercial Center, Moscow (in Russian).
Qin, S.J., Sun, Y.Z., Li, Y.H., Wang, J.X., Zhao, C.L., Gao, K., 2015. Coal deposits as promising alternative sources for gallium. Earth-Sci. Rev. 150, 95–101. https://doi.org/10.1016/j.earscirev.2015.07.010.
Rikhvanov, L.P.; Ershov, V.V.; Vertman, E.G.; Potseluev, A.A., Arbuzov, S.I., Sarnaev, S.I., Sudyko, A.F., Yazikov, E.G., 1992. Complex ecological-geochemical studies of the Siberian coals. Energy and environment: Proceedings of the International Conf. Russia Khabarovsk, 1992. 68-71. (in Russian).
Rikhvanov, L.P., Vertman, E.G., Ershov, V.V., Potseluev, A.A., Arbuzov, S.I., 1994. Complex mineralogical-geochemical research of the known and newly discovered deposits with the purpose of revealing non-traditional types of rare, rare-earth and noble metals: Abstracts of the best scientific developments at the competition of grants on fundamental researches in the field of geology. Moskow 23–24 (in Russian).
Seredin, V.V., 1994. The first data on abnormal concentrations of niobium in coals of Russia. Rep. Acad. Sci. 335 (5), 634–636 (in Russian).
Seredin, V.V., 2001. Main regularities of distribution of the rare-earth elements in coals. Dokl. Earth Sci. 377 (2), 239–243.
Seredin, V.V., 2004. Metal-bearing coals: conditions of formation and prospects of development. Coal base of Russia. Volume VI. Main regularities of coal formation and coal bearing capacity in Russia. Geoinformmark LLC, Moscow. (in Russian).
Seredin, V.V., 2012. From coal science to metal production and environmental protection: A new story of success. Int. J. Coal Geol. 90–91, 1–3. https://doi.org/10.1016/j.coal.2011.11.006.
Seredin, V., Dai, S., 2012. Coal deposits as potential alternative sources for lanthanides and yttrium. Int. J. Coal Geol. 94, 67–93. https://doi.org/10.1016/j.coal.2011.11.001.
Seredin, V., Dai, S., Sun, Y., Chekryzhov, I., 2013. Coal deposits as promising sources of rare metals for alternative power and energy-efficient technologies. Appl. Geochem. 31, 1–11. https://doi.org/10.1016/j.apgeochem.2013.01.009.
Seredin, V., Finkelman, R., 2008. Metalliferous coals: a review of the main genetic and geochemical types. Int. J. Coal Geol. 76, 253–289. https://doi.org/10.1016/j.coal.2008.07.016.
Shvartsev, S.L., Domrocheva, E.V., Rasskazov, N.M., 2011. Geochemistry and formation of soda waters of Kuzbass. Izvestiya Tomsk Polytech. Univ. 318 (1), 128–134 (in Russian).
Shvartsev, S.L., Lepokurova, O.E., Ponomarchuk, V.A., Domrocheva, E.V., Sizikov, D.A., 2016. Abnormal composition of carbon isotopes in underground alkaline waters of Kuzbass. Doklady Earth Sci. 469 (Part 2), 877–881. https://doi.org/10.1134/S1028334X16080286.
Solodov, N.A., Semenov, E.I., Burkov, V.V., 1987. Geological Reference Book on Heavy Lithophilic Rare Metals. Nedra, Moskow (in Russian).
Spears, D.A., 2012. The origin of tonsteins, an overview, and links with seatearths, fireclays and fragmental clay rocks. Int. J. Coal Geol. 94, 22–31. https://doi.org/10.1016/j.coal.2011.09.008.
Spears, D.A., Arbuzov, S.I., 2019. A geochemical and mineralogical update on two major tonsteins in the UK Carboniferous Coal Measures. Int. J. Coal Geol. 210, 103199. https://doi.org/10.1016/j.coal.2019.05.006.
Taylor, S.R., McLennan, S.M., 1985. The Continental Crust: Its Composition and Evolution. Blackwell Scientific, Oxford, London, Edinburgh, Boston, Palo Alto, Melbourne.
Taylor, J.C., 1991. Computer programs for standardless quantitative analysis of minerals using the full powder diffraction profile. Powder Diffract. 6, 2–9.
Titaeva, N.A., 2005. Geochemistry of the natural radioactive decay series. Moscow GEOS, 226 p (in Russian).
Vakh, E.A., Vakh, A.S., Kharitonova, N.A., 2013. The contents of rare earth elements in waters of hypergenesis zone of sulfide ores Gold Deposit (upper Amur region). Tikhookeanskaya Geologiya V 32 (1), 105–115.
Vergunov, A.V., Arbuzov, S.I., Sobolenko, V.M., 2019. Mineralogy and geochemistry of the tonsteins in the coals of the Beisk deposit of Minusinsky Basin. Bull. Tomsk Polytech. Univ. Geo Assets Eng. 330 (2), 155–166. https://doi.org/10.18799/24131830/2019/2/116. (in Russian). DOI.
White, J.C., Parker, D.F., Ren, M., 2009. The origin of trachyte and pantellerite from Pantelleria, Italy: Insights from major element, trace element, and thermodynamic modelling. J. Volcanol. Geoth. Res. 179, 33–55. https://doi.org/10.1016/j.jvolgeores.2008.10.007.
Winchester, J.A., Floyd, P.A., 1977. Geochemical discrimination of different magma series and their differentiation products using immobile elements. Chem. Geol. 20, 325–343.
Xin, F., Xu, H., Tang, D., Yang, J., Chen, Y., Cao, L., Qu, H., 2019. Pore structure evolution of low-rank coal in China. Int. J. of Coal Geol. 205, 126–139. https://doi.org/10.1016/j.coal.2019.02.013.
Yarmolyuk, V.V., Kozlovsky, A.M., Kuzmin, M.I., 2013. Late Paleozoic-early Mesozoic within-plate magmatism in north Asia: traps, rifts, giant batholiths, and the geodynamics of their origin. Petrology 21 (2), 101–126. https://doi.org/10.1134/S0869591113010062.
Yarmolyuk, V.V., Kozlovsky, A.M., Nikiforov, A.V., Travin, A.V., Lykhin, D.A., 2016. Composition, sources, and mechanisms of origin of rare-metal granitoids in the late Paleozoic Eastern Sayan zone of alkaline magmatism: a case study of the Ulaan Tolgoi massif. Petrology 24 (5), 477–496. https://doi.org/10.1134/S0869591116050064.
Yegyan, M.O., Rozhanets, A.V., 2008. In: Usova, T.Yu (Ed.), Tantalum,Rare metals: the world market. Book.I. Metals produced from the own deposits. Beryllium, Germanium, Lithium, Niobium, Rare-earths, Strontium, Tantalum, Cesium, Zirconium. IMGRE, Moskow, pp. 125–149 (in Russian).
Yudovich, Ya.E., Ketris, M.P., 2002. Inorganic substance of coals. Ural Branch of RAS Yekaterinburg. (in Russian).
Yuzvitsky, A.Z., 2003. Kuznetsk coal basin. Coal Base of Russia. Vol. II. The Coal Basins and Deposits in Western Siberia(Kuznetsky, Gorlovsky, West Siberian, Basins and Deposits of the Altai Krai and the Altai Republic). Geoinformmark Publ., Moscow (in Russian).
Zhao, C., Liu, B., Xiao, L., Li, Y., Liu, S., Li, Z., Zhao, B., Ma, J., Chu, G., Gao, P., Sun, Y., 2017. Significant enrichment of Ga, Rb, Cs, REEs and Y in the Jurassic No. 6 coal in the Iqe Coalfield, northern Qaidam Basin, China –A hidden gem. Ore Geol. Rev. 83, 1–13. https://doi.org/10.1016/j.oregeorev.2016.12.012.
Zhao, L., Dai, S., Graham, I.T., Li, X., Liu, H., Song, X., Hower, J.C., Zhou, Y., 2017a. Cryptic sediment-hosted critical element mineralization from eastern Yunnan Province, southwestern China: mineralogy, geochemistry, relationship to Emeishan alkaline magmatism and possible origin. Ore Geol. Rev. 80, 116–140. https://doi.org/10.1016/j.oregeorev.2016.06.014.
Zhao, L., Zhu, Q., Jia, S., Zou, J., Nechaev, V., Dai, S., 2017b. Origin of minerals and critical metals in an argillized tuff from the Huayingshan Coalfield, southwestern China. Minerals 7, 92. https://doi.org/10.3390/min7060092.
Zhou, Y., Bohor, B.F., Ren, Y., 2000. Trace element geochemistry of altered volcanic ash layers (tonsteins) in Late Permian coal-bearing formations of eastern Yunnan and western Guizhou Province. China. Int. J. Coal Geol. 44, 305–324. https://doi.org/10.1016/S0166-5162(00)00017-3.
Zhuang, X., Querol, X., Alastuey, A., Juan, R., Plana, F., Lopez-Soler, A., Du, G., Martynov, V.V., 2006. Geochemistry and mineralogy of the Cretaceous Wulantuga high-germanium coal deposit in Shengli coal field, Inner Mongolia, Northeastern China. Int. J. Coal Geol. 66, 119–136. https://doi.org/10.1016/j.coal.2005.06.005.